STANFORD RSL Technical Report 69-2

QUANTITATIVE GEOLOGIC ANALYSIS OF MULTIBAND PHOTOGRAPHY FROM THE MONO CRATERS AREA, CALIFORNIA

by

Gary I. Ballew*
Geology Department
School of Earth Sciences
Stanford University
Stanford, California

February 1969

*Now at Bendix Corporation, Ann Arbor, Michigan

REMOTE SENSING LABORATORY
SCHOOL OF EARTH SCIENCES
STANFORD UNIVERSITY • STANFORD, CALIFORNIA

STANFORD RSL Technical Report 69-2

QUANTITATIVE GEOLOGIC ANALYSIS OF MULTIBAND PHOTOGRAPHY FROM THE MONO CRATERS AREA, CALIFORNIA

by

Gary I. Ballew *
Geology Department
School of Earth Sciences
Stanford University
Stanford, California

Already Issued

67-1 "Field Infrared Analysis of Terrain - Spectral Correlation Program" Part I

67-2 "Field Infrared Analysis of Terrain - Spectral Correlation Program" Part II and Part III

67-3 "Statistical Analysis of IR Spectra - Stanford Programs Applied to USGS Spectra in Tech Letter #13"

67-4 "Computer Reduction and Analysis of an Infrared Image"

68-1 "Infrared Exploration for Coastal and Shoreline Springs"

68-2 "Re-evaluation of the Normative Minerals of Sonora Pass Rock Standards - Univ. Nev. Reports #7 and #12"

68-3 "Nearest Neighbor - A New Non-Parametric Test Used for Classifying Spectral Data".

Final Report "Field Analysis of Terrain" - NGR-05-020-115 (contains all the drawings and logic diagrams for Stanford CVF Spectrometer and Digital Data Recording System.

69-1 "Mission 78 - Flights 1 and 2 Ninety Day report

*Now at Bendix Corporation, Ann Arbor, Michigan

This research report was submitted to the Department of Geology of Stanford University in partial fulfillment of the requirements for the Degree of Master of Science, March 1968. Partial support was provided under NASA Grant NGR-05-020-115 and NASA Contract NAS9-7313 in the Stanford Remote Sensing Laboratory.

R.J.P. Lyon
Principal Investigator

DISTRIBUTION LIST

NASA-WASHINGTON	No. of Copies
J.R. Porter	1
T.A. Geogge	1
Winnie Morgan	1
C. Centers	1
NASA-HOUSTON	
J.E. Dornbach	1
R.L. Duppstadt	1
Charles M. Grant (Data Bank)	5
W.E. Hensley	1
Ed Zeitler	1
NASA-CAMBRIDGE	
Glen Larson	1
USGS	
Bob Alexander	1
W.D. Carter	1
R.W. Fary	1
W.H. Hemphill	1
USDA	
V. Myers	1
Arch Park	1
USNOO	
H. Yotko	1
Others	
F. Barath	1
Branner Library	1
Engineering Library	1
R.N. Colwell	1
DAve Landgrebe	1
J. Quade	1
Ralph Shay	1
Dave Simonett	1
Don Walsh	1
E.W.T. Whitten	1

<u>TABLE OF CONTENTS</u>

LIST OF ILLUSTRATIONS

LIST OF TABLES

I. INTRODUCTION

The primary purpose of this report is to determine the effectiveness of remote sensing techniques in geologic mapping applications. This was accomplished by selecting an area of previously mapped geology and analyzing it with all remote sensing data available. The area selected for study was the northern portion of the Mono Craters, Mono County, California, primarily because data of all the major wavelength regions were available when research for this report began in September, 1966. Specific areas of interest were field checked and samples collected in April, August and October of 1967 in attempts to correlate local geology with aircraft data, using quantitative analytical approaches.

I would like to acknowledge the assistance provided by Dr. R. J. P. Lyon, who was responsible for obtaining the basic National Aeronautics and Space Administration remote sensing data and advising in its interpretation. Only the multiband photographic data from the area was analyzed in great detail. Radar and infrared scanner data were also studied but not in the depth required for quantitative geologic evaluation.

The portion of the Mono Craters studied in this report is located in the northeastern quadrant of the Mono Craters 15-minute quadrangle and includes the area from the south shore of Mono Lake to about Crater Mountain, near the center of the main arc of the Mono Craters. This area is from three to five miles east of the frontal scarp of the Sierra Nevada and is on the border between the Sierra Nevada and Basin and Range physiographic provinces. Topographic relief of the craters above the surrounding pumice plains varies from 200 feet at North Crater, to 2000 feet at Crater Mountain (Figure 1). All major streams in the area originate in the Sierras and flow into Mono Lake, a highly saline body of water which has no external drainage. Water from rain or snowfall in the craters drain into the sparsely vegetated and porous areas of pumice and does not produce significant surface drainage. There are also areas of springs along the shore of Mono Lake, some of which are hot springs.

The climate of this region is arid to semi-arid and supports little vegetation in areas of rock outcrop, other than lichen and a few widely scattered pine trees. Regions of pumice surround these outcrops, and may vary from essentially unvegetated on steep slopes, to dense growths of sagebrush in areas of gently-sloping topography. Other locations of little or no vegetation include deposits of beach sand and formations of calcareous tufa along the shore of the lake. This combination of sparse vegetation, distinctive terrain types, and available data has provided an excellent area for geologic remote sensing investigations.

II. GEOLOGY

The regional geology of the Mono Craters area consists of a basement complex of metamorphosed Paleozoic and Mesozoic sedimentary and volcanic rocks and Mesozoic granitic rocks. This was demonstrated by Kistler (1966), who also states that the granitic rock is composed chiefly of granodiorite and quartz monzonite and occurs in plutons of moderate size. This complex is covered by Tertiary and Quaternary volcanic rocks and Quaternary lake sediments, moraines, pumice deposits and alluvium.

The geologic units studied are all of Recent age, including the flows of the main crater complex. This was indicated in work done by Kistler (1966) and Friedman (1966), and emphasizes the extremely youthful age of these units. The arcuate form of the main crater complex has suggested that this is a portion of a ring-fracture zone that formed after the Sherwin Glaciation and before the eruption of the Bishop Tuff (Kistler, 1966).

The geologic maps used in this report are all derived from Friedman's compilation of mapping done in the area, as they provide the most detailed information available (Fig. 2 and 3).

III. ANALYSIS OF VISUAL AND NEAR INFRARED FIELD SPECTRA*

Although reflectance spectras are available in the visible and near infrared region from 0.4 to 1.5 microns, there is very little data of a geological nature which can be used for field analysis. This situation is especially evident when analyzing the remote sensing data presently available in the form of multiband photography from Mono Craters, California. This is currently being studied in an attempt to perfect a method of multi-spectral geologic mapping.

The field spectra presented here were obtain at North Crater (sometimes known as Panum Crater), a rhyolite, obsidian and pumice explosion crater approximately one-half mile in diameter and rising 200 to 300 feet above a plain of moderately vegetated pumice. It is located about a mile south of Mono Lake and is a northern extension of the main arc of the Mono Craters (See Fig. 1 and 2).

Although the conditions for obtaining on-site reflectance spectra on April 1, 1967 were not ideal, the methods employed were as consistent as possible and agree with spectra collected during August, 1967.

An ISCO spectro-radiometer fitted with a fiber-optics, remote probe was used to obtain these spectra, which ranged in wavelength from 0.425 to 1.55μ. The <u>reflectance</u> at each wavelength was calculated by taking the ratio of reflected to total intensity, both intensities being measured over a 180° (2π steradian) field of view.

---

*From: Semi-Annual Report dated 15 May 1967, "Field Infrared Analysis of Terrain", NASA Grant NGR-05-020-115.

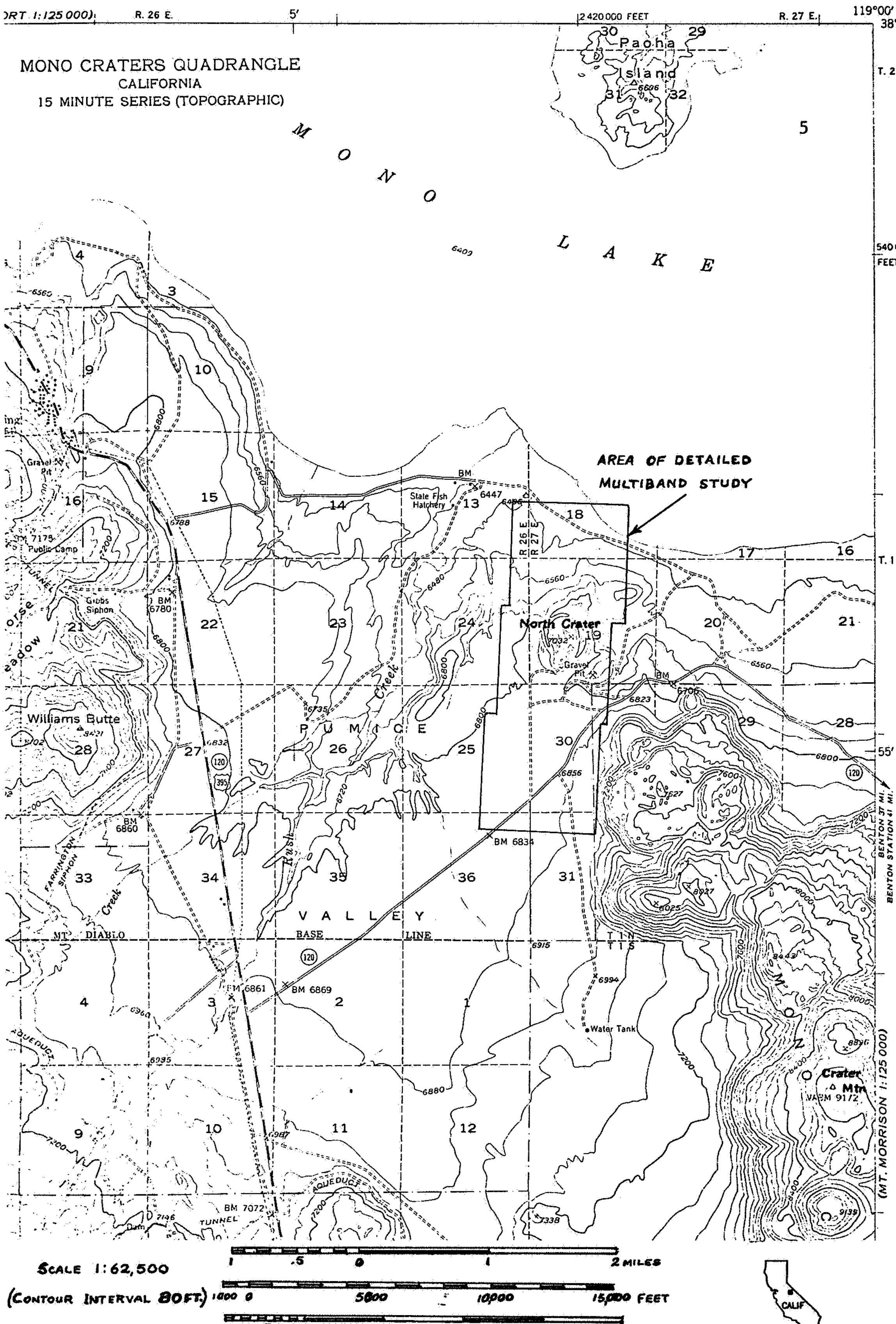
MONO CRATERS QUADRANGLE
CALIFORNIA
15 MINUTE SERIES (TOPOGRAPHIC)
R. 26 E.
R. 27 E.
119°00′
38°00′
2 420 000 FEET
540 000 FEET
T. 2 N.
T. 1 N.
Paoha Island
MONO LAKE
AREA OF DETAILED MULTIBAND STUDY
State Fish Hatchery
North Crater
Gravel Pit
Williams Butte
PUMICE VALLEY
Rush Creek
MT. DIABLO BASE LINE
Gibbs Siphon
Farrington Siphon
Public Camp
Water Tank
Aqueduct
Tunnel
Crater Mtn
MONO
BENTON 37 MI.
BENTON STATION 41 MI.
(MT. MORRISON 1:125 000)
SCALE 1:62,500
(CONTOUR INTERVAL 80 FT.)
2 MILES
15,000 FEET
4 KILOMETERS
CALIF
QUADRANGLE LOCATION

FIGURE I

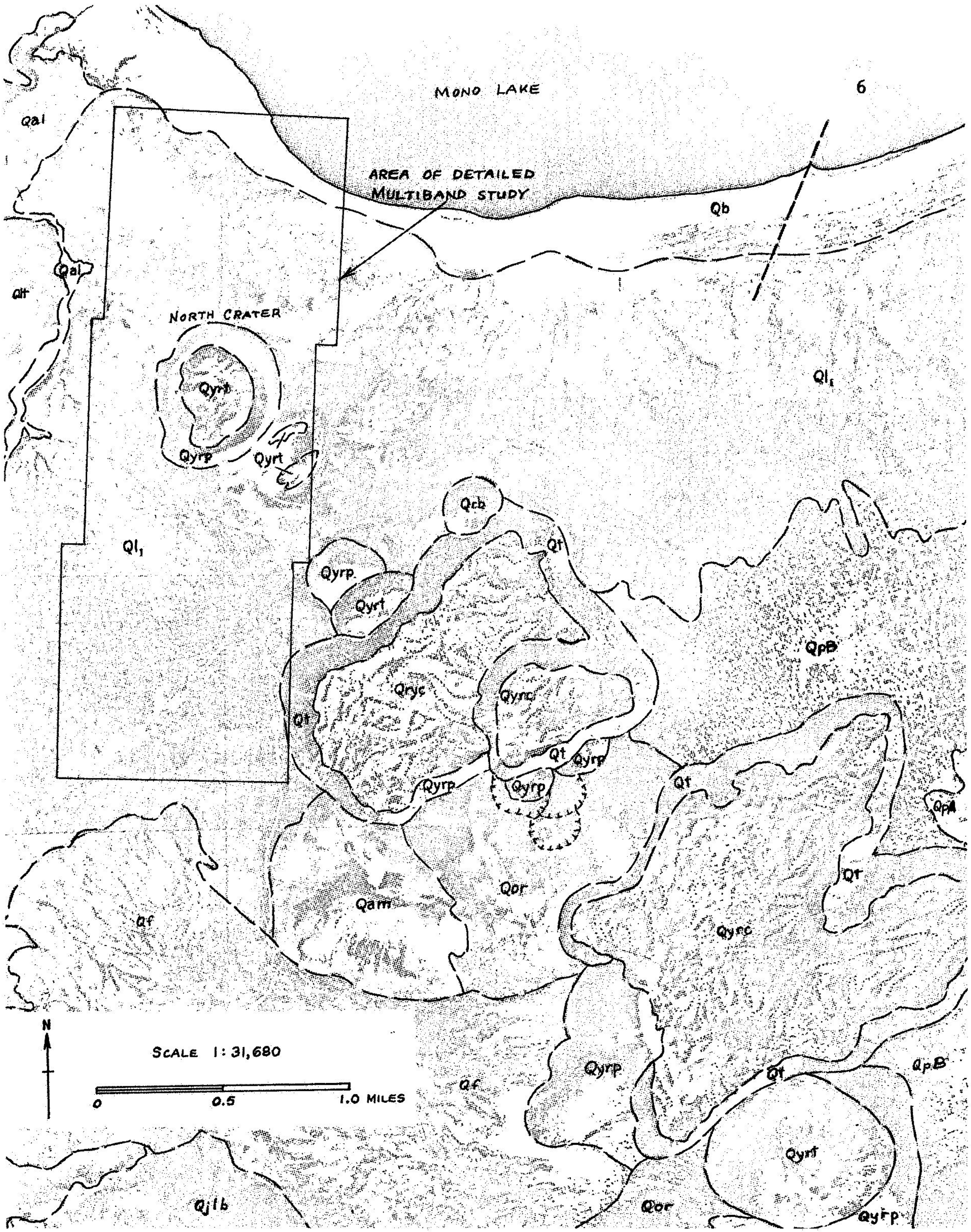

PHOTOGEOLOGIC MAP OF THE NORTHERN MONO CRATERS, CALIFORNIA

After J. D. Friedman, 1966

Figure 2

GEOLOGIC COLUMN TO ACCOMPANY PHOTOGEOLOGIC MAP OF NORTHERN MONO CRATERS AREA, CALIFORNIA

AGE	SEDIMENTARY UNITS		IGNEOUS UNITS	
RECENT	Qb	BEACH DEPOSITS OF MONO LAKE INCLUDING CALCAREOUS TUFA AND DELTAIC DEPOSITS.		
	Qt	SLIDEROCK AND TALUS OF COULEE FRONT.		
	Qf	FAN AND SLOPEWASH DEPOSITS		
	Qal	STREAM AND OTHER ALLUVIAL DEPOSITS INCLUDING REWORKED ASHFALL DEPOSITS.		
	Qlt	DISSECTED STREAM-CUT TERRACES IN LACUSTRINE DEPOSITS WITH SOME Qal.		
			QpA	~~PUMICE TEPHRA (ASH AND LAPILLI)~~ ASHFALL VENEER AND BARREN PUMICE SANDFLATS.
			QpB	SAME AS QpB BUT WITH VEGETATION AND MINOR RELIEF.
			Qyrc	YOUNGER PUMICEOUS RHYOLITE OBSIDIAN OF COULEES.
			Qyrt	YOUNGER RHYOLITE AND OBSIDIAN OF VOLCANIC DOMES IN PLACES WITH OVERLYING Qyrp.
			Qrb	YOUNGER OBSIDIAN AND RHYOLITE OF BLOCK CRATERS.
			Qyrp	YOUNGER TEPHRA (LAPILLI & ASH) RINGS, RAMPARTS AND CONES.
	Ql_1	LACUSTRINE DEPOSITS INCLUDING OLDER DELTAIC GRAVELS & OVERLYING Qyrp EAST AND SOUTHEAST OF NORTH CRATER.		
			Qor	OLDER RHYOLITE DOMES AND FLOWS.
			Qam	ANDESITE OF MONO CRATERS.
			Qjlb	BASALT OF JUNE LAKE JUNCTION

MAP SYMBOLS:

FLOW RIDGES ON COULEE SURFACES, TREND GENERALLY TRANSVERSE TO DIRECTION OF MOVEMENT.

EXPLOSION CRATERS OR VENTS IN PYROCLASTIC DEPOSITS, RHYOLITE OR ANDESITE-BASALT EXTRUSIVES.

CONTACTS

INFERRED FAULTS

FIGURE 3

As this is a completely portable instrument, spectra of samples were taken in place and the samples collected for further study. Of the twenty wavelengths used, nine correspond to the filtered bands of the multiband camera.

When these reflectance values (Table I) are plotted against wavelength (Fig. 4) we notice that most of the variation occurs in the visible region from 0.425 to 0.750μ and that, with the exception of black obsidian, the highest reflectance occurs in the near infrared. The two samples of gray obsidian are both from the Mono Craters area, but the one showing highest spectral reflectance is from a sample provided for field analysis by the University of Nevada's NASA Project. Both of these spectra are similar below 0.575μ (violet to yellow light), but become less similar at wavelengths greater than this. Note particularly the higher overall intensity of the rough gray obsidian relative to the smooth one. This may be caused by the rough surface of the first obsidian, apparently is more reflectant than the smooth surface of the other sample.

The spectrum of black obsidian is uniform and unexpectedly high over much of the visual region with reflectance reaching a minimum in the infrared. The smooth surface of this obsidian block helps to explain its high reflectance, as the sun was at a very low angle and the outlet was on a steep slope facing the sun.

The spectrum of red rhyolite shows very low reflectance in the shorter wavelength visible region, with an expected maximum in the 0.75μ (red) region. This high reflectance persists into

TABLE I

VISUAL AND NEAR INFRARED FIELD DATA

FROM MONO LAKE AREA, CALIFORNIA

Reflectance, %;

wavelength, microns	gray rough obsidian*	gray smooth obsidian	black smooth obsidian	red smooth rhyolite	pumice soil
0.425	14.9	10.3	11.4	5.7	8.8
0.475	14.5	13.0	13.3	6.7	10.2
0.525	15.2	14.0	12.9	7.6	10.7
0.575	16.7	14.6	12.9	11.4	12.2
0.625	20.3	16.0	12.5	15.6	12.9
0.675	21.4	15.8	15.6	16.7	14.2
0.725	25.6	18.3	17.0	17.7	14.6
0.800	25.9	17.5	14.3	18.7	--
0.850	25.0	17.5	16.0	18.6	--
0.950	27.5	17.7	11.1	20.0	--
1.050	27.8	16.7	11.8	20.0	--
1.150	29.1	17.0	11.0	20.8	--
1.250	26.3	15.9	11.1	20.0	--
1.350	26.7	17.4	14.3	20.6	--
1.450	25.9	17.0	12.7	17.0	--
1.550	23.0	16.3	13.7	17.9	--

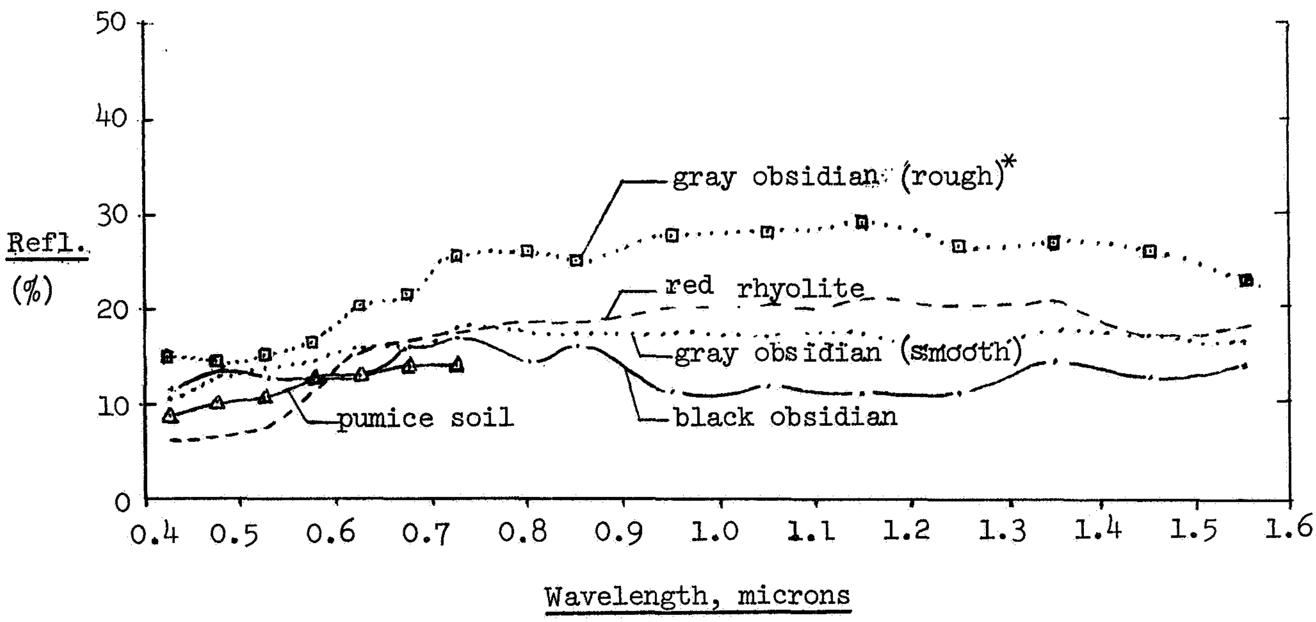

REFLECTANCE SPECTRA

Figure 4

* Sample collected by Univ. of Nevada NASA Project.

the infrared and shows little variation except at very long wavelengths. In contrast, the pumice soil spectrum shows higher values in the violet and lower values in the red regions of the visual, with a crossover near 0.60μ (orange). The pumice spectrum does not extend into the infrared, as time did not permit its completion.

A characteristic of all the longer wavelength infrared spectra is their tendency to converge toward the same reflectance in the region near 1.55μ, with no crossovers occurring in the entire near infrared region. Combining this information with that obtained in the visual portion, we note that there are a number of optimum* wavelengths which could be used for rock spectra classification. In the visible these are 0.425μ (violet), 0.475μ (blue), and 0.725μ (red), with 0.80μ in the photographic infrared and 0.90 to 1.35μ and 1.5μ in the region beyond photographic detection. Thus, by using these bands, the non-vegetated areas near Mono Craters could be classified as red rhyolite, black obsidian, gray obsidian or pumice. Hopefully, other areas of similar lithology and vegetation cover could be mapped using presently available data in the area around Mono Lake. This assumes, of course, that repeatable reflectance spectra could be obtained under other field conditions. Clearly this would form the foundation of any future research.

---

*Optimum: Defined as those wavelengths at which relative maximum or minimum reflectance values occur.

IV. MULTIBAND GEOLOGIC ANALYSIS

A. System Description:

This system is designed to gather information in the visible and near or short wavelength infrared region of the electromagnetic spectrum by means of nine combinations of films and filters. The nine-lens camera (Fig. 5) accomplishes this by simultaneously exposing three frames of each of three rolls of film as the aircraft flies over the terrain to be "sensed". Two of these films are conventional panchromatic (black-and-white) film, while the third is infrared black-and-white film (Fig. 6).

Unfortunately, the roll of infrared film for this flight was spoiled in the developing process and only the six visual filter combinations, or "bands" were able to be studied.* The wavelengths of visual light recorded by these bands correspond roughly to the colors violet, blue, green, yellow, orange, and red--in order of band-number from one to six (Fig. 7). Even with the drawback of not having the infrared bands, it is still clearly possible to obtain meaningful data from visual film and will serve as a demonstration of a general method of multi-spectral analysis.

Of the approximately sixty sets (each set consists of six spectral bands) of exposures which were taken over the region near Mono Lake, three sets of six spectral bands were chosen because they showed a diversity of features. As this flight was

*The Mono Craters area had only been flown once with the NASA 9-lens camera prior to January 1, 1968.

Itek Nine-Lens 70-mm Camera, Model 2.

(From NASA Anthology, 1966)

Figure 5

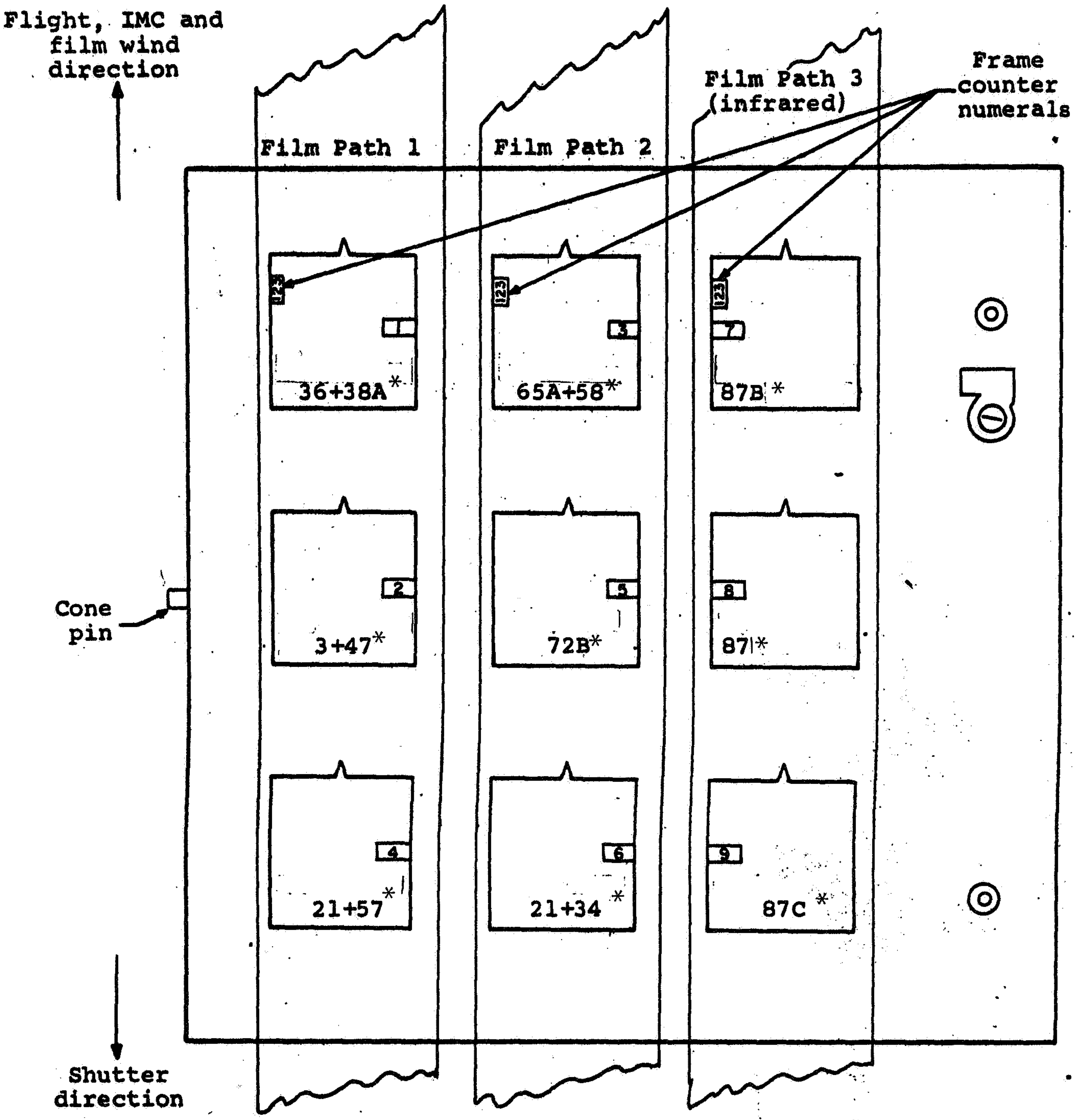

* Wratten filter combinations

Schematic view of format area nine-lens camera model 2.

(From NASA Anthology, 1966)

Figure 6

IMPORTANT PARAMETERS FOR MULTIBAND PHOTOGRAPHY

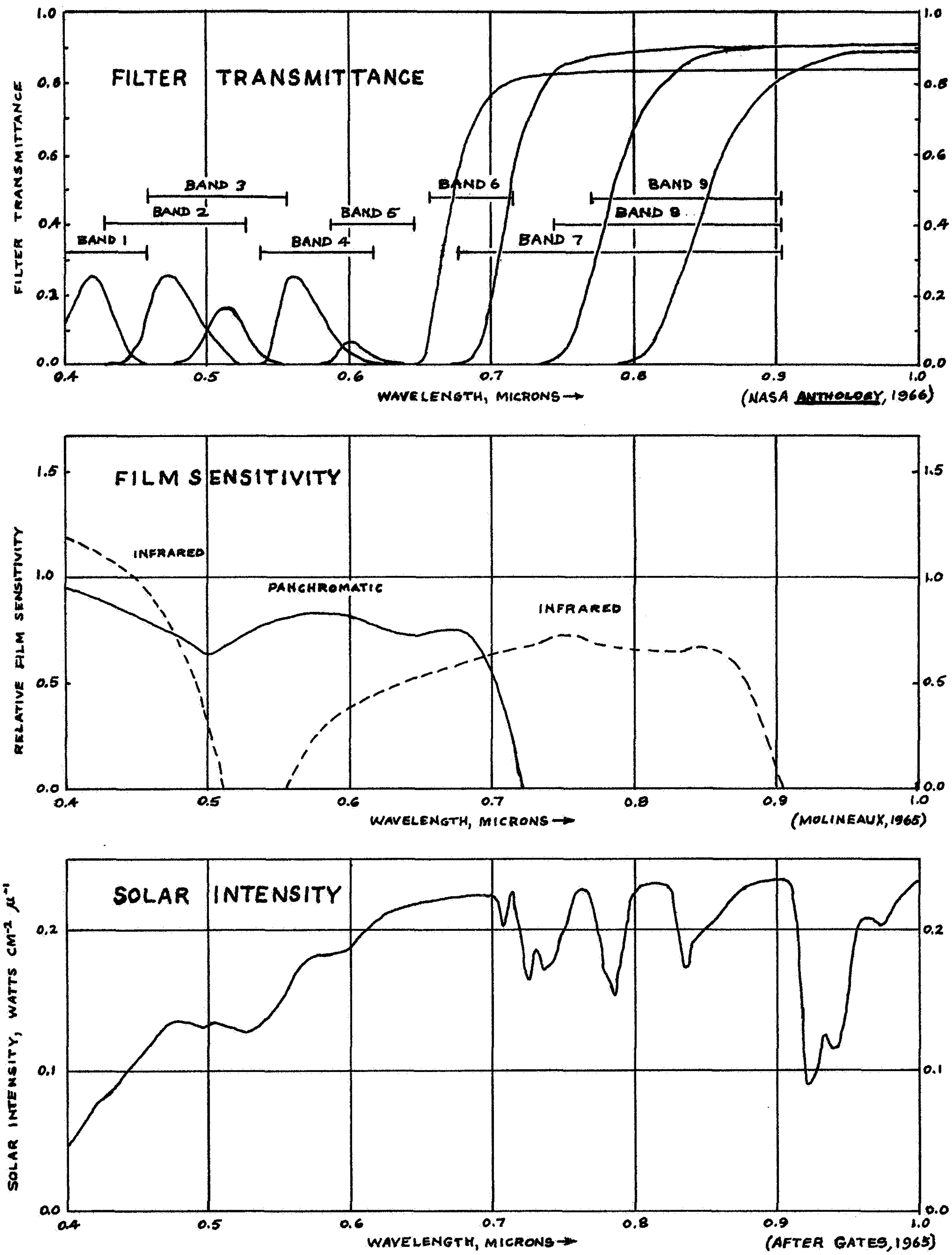

Figure 7

flown at about 9:00 A.M. on September 30, 1965, there were several areas of shadow which also served as another potential type of feature for classification. The three sets of photographs show adjacent areas along a north-south distance of about three miles, with the average width of each photograph being about one mile and overlap amounting to less than 10 percent on each. The northern-most photograph shows a portion of the south shore of Mono Lake, a strip of beach deposits, and an area of varying amounts of pumice sand and sagebrush, while the middle photo contains a small rhyolite and obsidian dome surrounded by a plain of pumice vegetated with sagebrush and crossed by roads. The southern-most photo also shows an area of pumice sand covered with sagebrush and crossed by California Highway 120.

B. Data Acquisition:

Having selected the areas to be studied, the next step was to find a satisfactory method of obtaining "gray scale" or, as these were transparencies, the transmittance values from each of the 18 exposures. After experimenting with several densitometers, the Jarrel-Ash Recording Spectrographic Densitometer was chosen for its sensitivity, film positioning accuracy, and the permanent record of transmittance values which it records on chart paper. With this instrument five profiles of transmittance were obtained along north-south lines spaced 10 mm apart and centered about the middle of each exposure. The graphical output of the densitometer was then digitized at intervals equivalent to 5 mm on the film, with this being done for each of the five profiles obtained from each of the 18 photos (Fig. 8). There were nine of these data points on each of the profiles, so that no measurements were taken closer than 10 mm from the edges of the positives--in the region of abnormally high film transmittance. The photographs used for Figures 9 and 10 are rejected duplicates and are used for illustration purposes only. The original transparencies are to be used in further experiments and were not cut apart for illustration purposes.

Having obtained five profiles of nine points each, for a total of 45 points per transparency, additional data was obtained from the central north-south profile over North Crater from forty points spaced at 1 mm intervals for use in one of the later methods of analysis. The first method of analysis required the use of only the three sets of 45 points for a total of 135 data points, each covering a field of view of 0.3 by 0.5 mm and representing six filtered bands. Each of these transmittance values were recorded on computer data cards in groups of six bands per location preceded by a coded description of the geology and vegetation as decided by ground inspection and photographic interpretation.

C. Methods of Analysis:

There were three primary methods of analysis used on this data, with each method being an attempt to discriminate the various terrain, geology, vegetation and lighting types present in the area covered by each of the photos. These three methods

PHOTOGRAPH GRID SYSTEM

DIMENSIONS:

	MM. ON PHOTO	FEET ON GROUND
DENSITOMETER SAMPLE SIZE	0.3 x 0.5	21 x 45
SAMPLE SPACING:		
OVERALL GRID	5.0 x 10.0	450 x 900
CENTERLINE	1.0	90

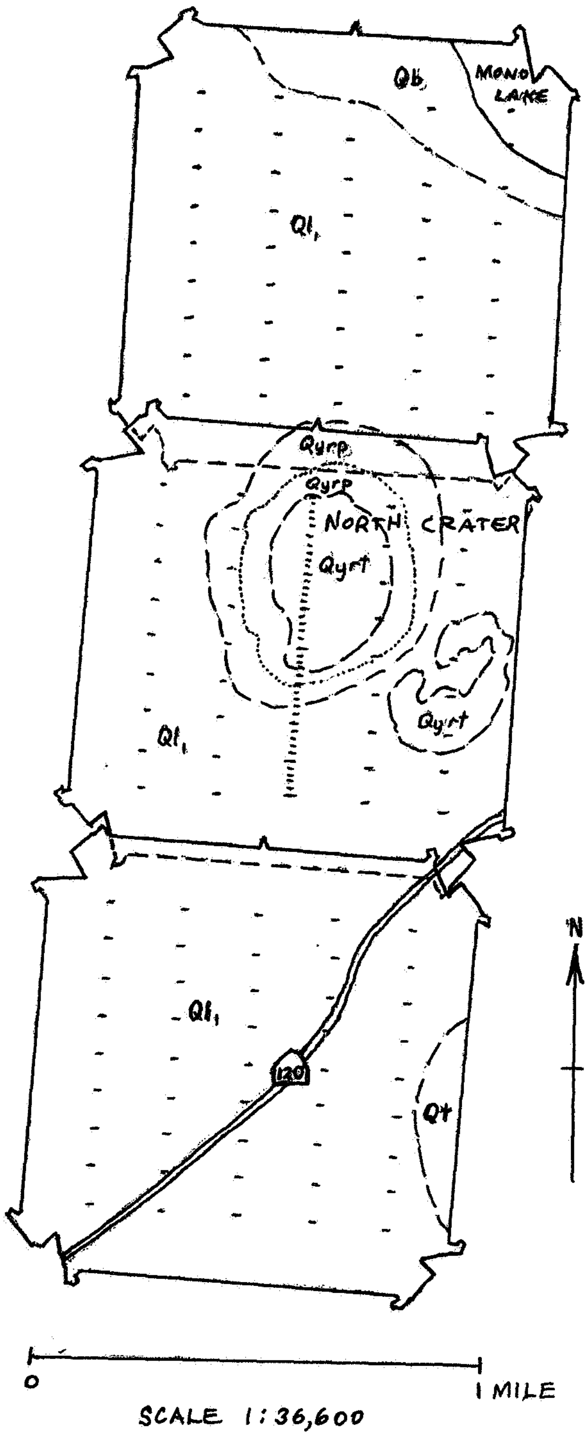

GEOLOGIC UNITS:

Qb - BEACH DEPOSITS.

Qt - SLIDEROCK AND TALUS.

Qyrt - YOUNGER RHYOLITE AND OBSIDIAN DOME.

Qyrp - YOUNGER TEPHRA

Ql_1 - LACUSTRINE DEPOSITS INCLUDES OLDER DELTAIC GRAVELS AND OVERLYING Qyrp NEAR NORTH CRATER.

120 - CALIFORNIA HIGHWAY 120

CONTACTS

CRATER RIM

SAMPLE AREAS

FIGURE 8

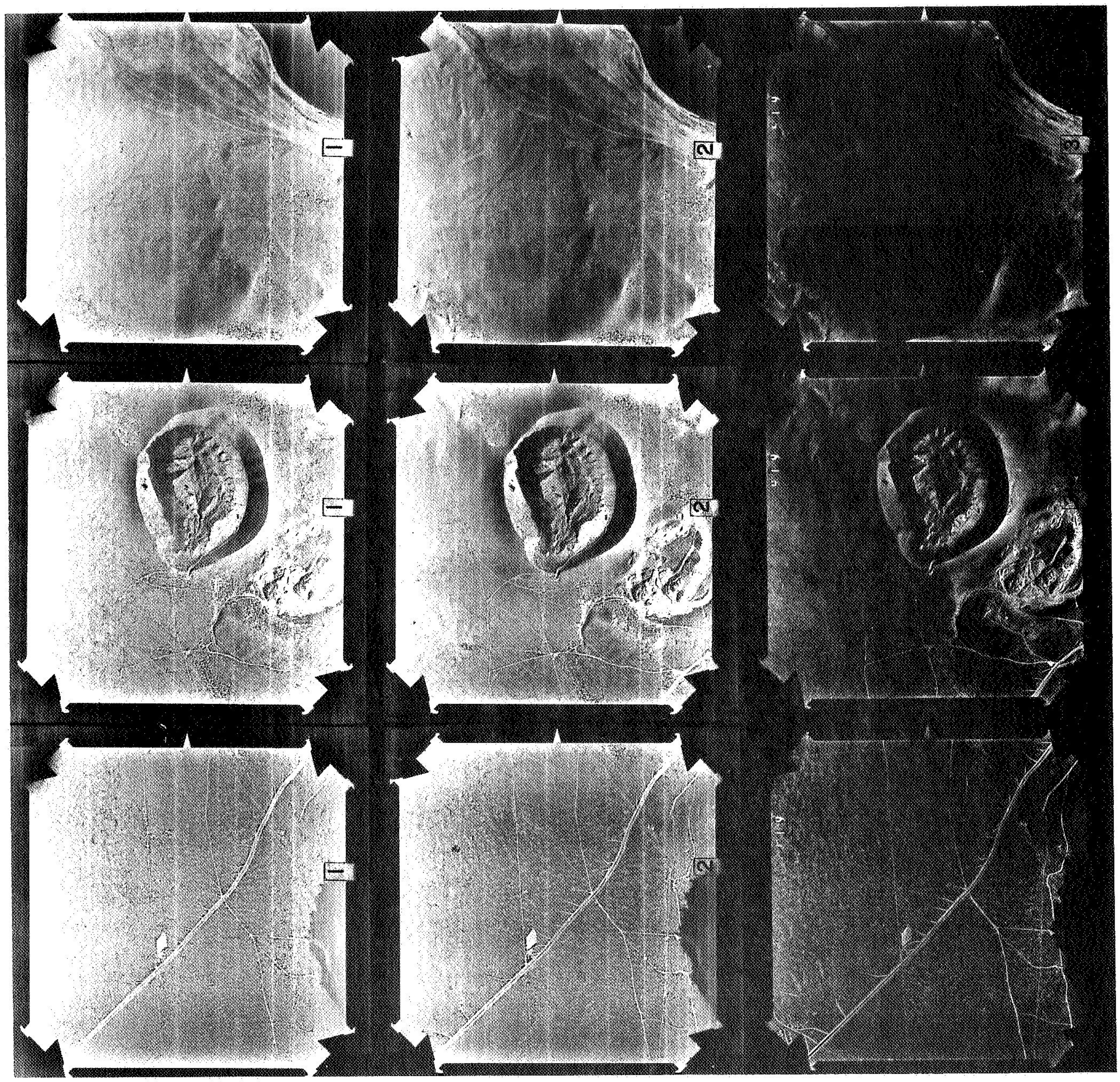

BAND 1	BAND 2	BAND 3
0.355 - 0.460 μ	0.430 - 0.530 μ	0.460 - 0.560 μ

Figure 9

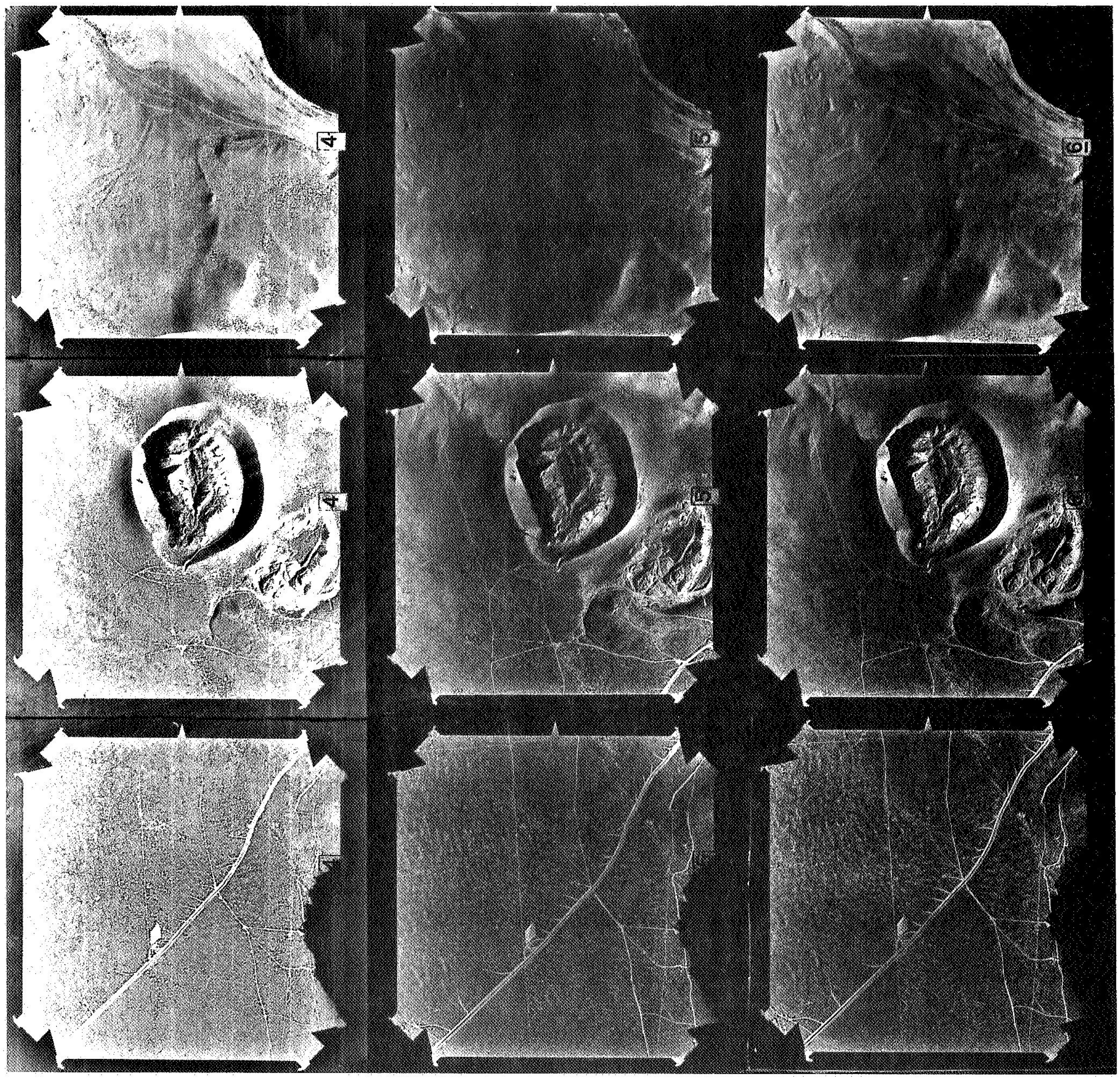

BAND 4 0.540 - 0.630μ

BAND 5 0.590 - 0.650μ

BAND 6 0.640 - 0.720μ

Figure 10

may be classed as investigations of trend surfaces, six-dimensional distances, and statistical models. The trend surfaces were the first to be studied and in general they were least valuable in discriminating terrain types, perhaps because only the trend surfaces themselves were studied and not the residual values of the transmittance data.

1. Trend Surfaces

In order to apply the method of trend surfaces to the multiband data, each wavelength of light was assumed to have its relative reflectance from the ground proportional to the transmittance values obtained from the photography. This is not necessarily correct, as solar intensity varies with wavelength and even this reflected energy is approximately proportional to the film density of the negative, where density = $\log_{10}$ (1/transmittance). This also assumes that the terrain being investigated is of uniform nature and does not consider variations in slope, surface irregularities, or minor vegetation changes. Variations from one site to another may be influenced by changes in sun angle, aircraft altitude, atmospheric transmission and cloud cover, as well as variations in film condition and processing.

Having made the assumption that reflectance is related to film transmittance, the 45 transmittance values on each of the three sets of six bands were fitted to a second degree trend surface (Harbaugh, 1964) of the form $Z = AX^2 + BXY + CY^2 + D$; where Z is the value of the transmittance in percent, X and Y are the coordinates of the point in millimeters from the upper left-hand corner of the photo, and A, B, C and D are the coefficients. When the resulting computer print-out trend contours were examined (Figures 11 and 12), most geologic discrimination was shown by band six, or red light. Even this did not bring out the exact location of the crater in the middle photo,* but did delineate the shore of Mono Lake fairly well. Another drawback of these trend surfaces is that they are not in alignment at photograph boundaries, even assuming 10 percent overlap.

A second method of trend surface analysis was used when the value of each of the spectral bands at each geographic point was compared to the mean of all six band transmittances. The formula for this was $DEV = \frac{TRANS}{MEAN} - 1$; where DEV is the positive or negative value of the transmittance of one of the six bands when compared to the average of all the bands at that point, TRANS is the transmittance of the band under study, and MEAN is the mean of all six bands at the point of interest. An intermediate program was written to make this computation and punch the six values of DEV on one card per "spectrum". Trend surfaces of these photographs were then contoured using the second-degree function in the above example, with much the same results (Fig. 13, 14). Once again the red wavelengths showed most discrimination.

2. Six-dimensional distances

The second major method of analysis assumed that if an area could be divided into several general terrain and geology

---

*Compare Fig. 11 with Fig. 9, and Fig 12 with Fig. 10 etc.

SECOND DEGREE TREND SURFACES FITTED TO 45

MULTIBAND FILM TRANSMITTANCE VALUES PER PHOTO

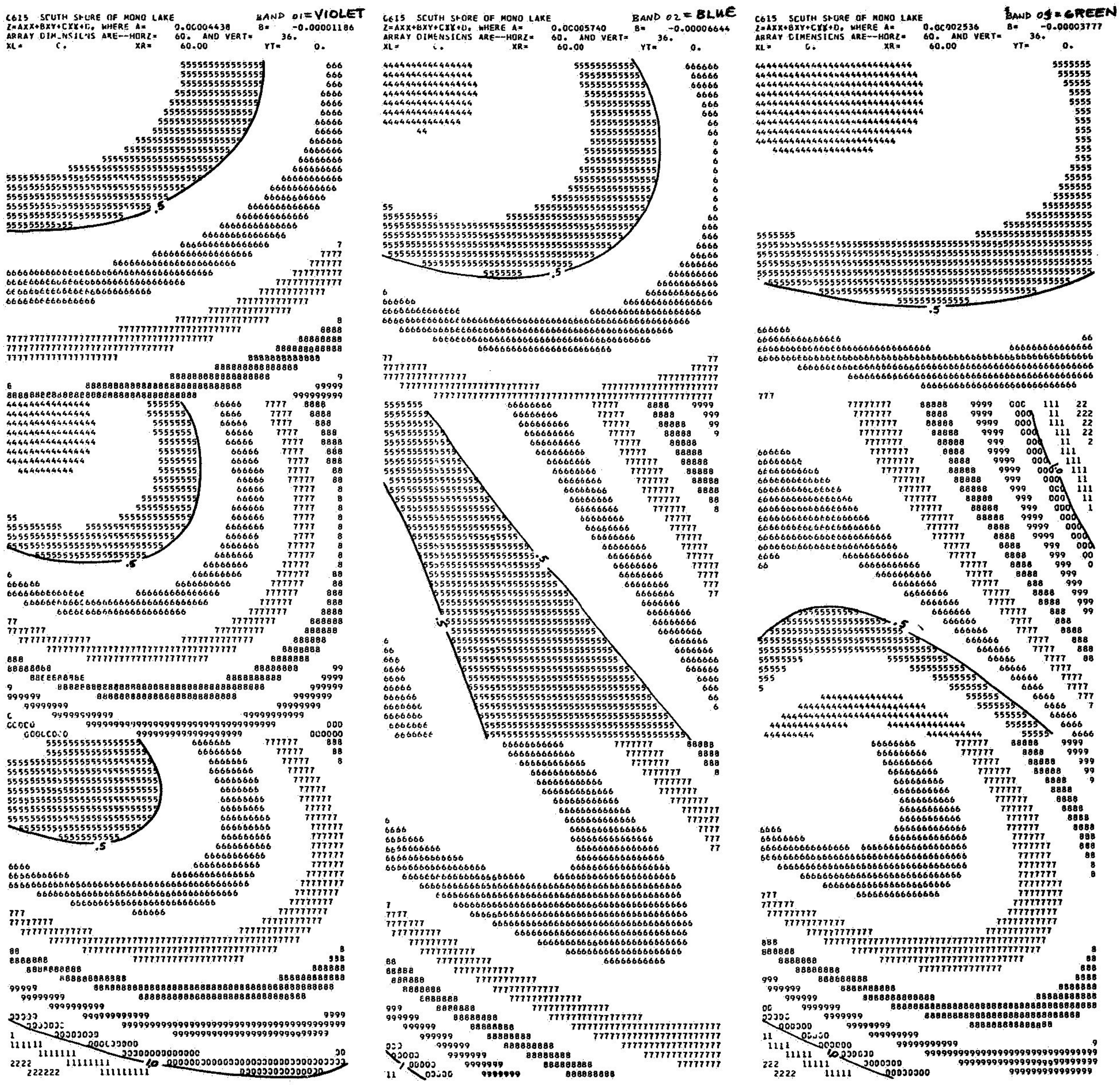

BAND 1 BAND 2 BAND 3

Figure 11

SECOND DEGREE TRENL SURFACES FITTED TO 45

MULTIBAND FILM TRANSMITTANCE VALUES PER PHOTO

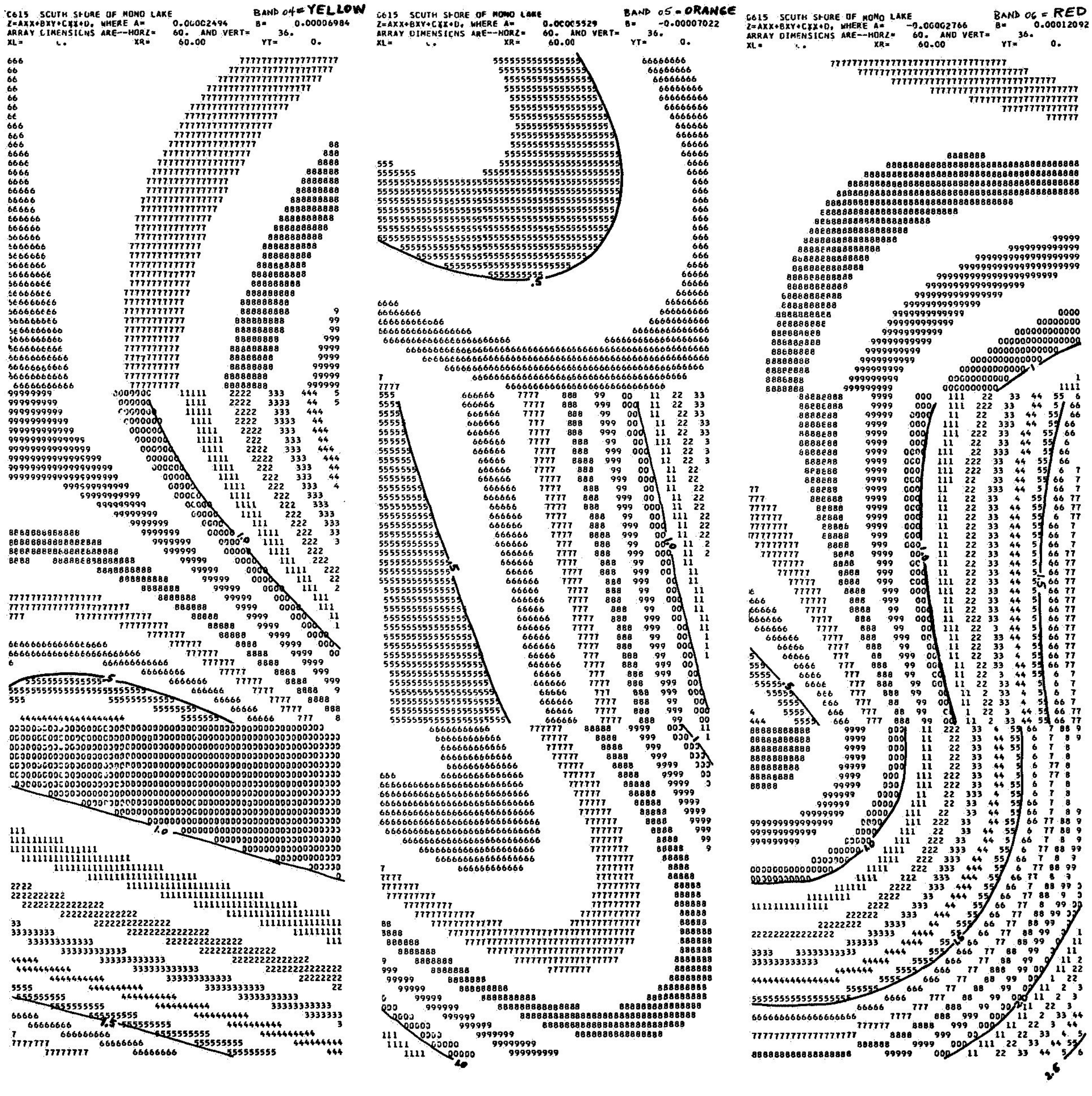

BAND 4 BAND 5 BAND 6

Figure 12

SECOND DEGREE TREND SURFACES FITTED TO DEVIATION FROM AVERAGE MULTIBAND FILM TRANSMITTANCE

(45 VALUES PER PHOTO)

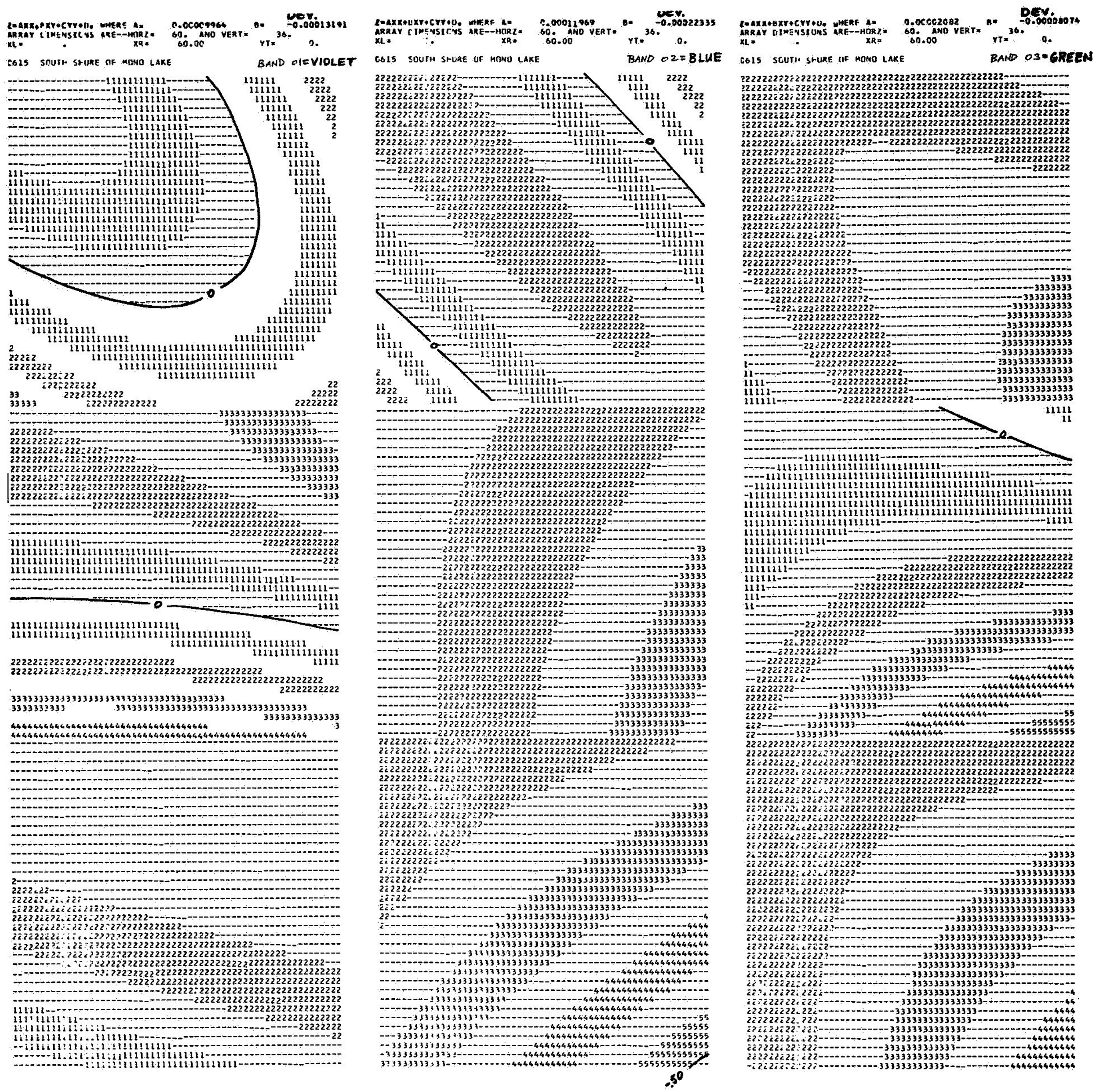

BAND 1 BAND 2 BAND 3

Figure 13

SECOND DEGREE TREND SURFACES FITTED TO DEVIATION FROM AVERAGE MULTIBAND FILM TRANSMITTANCE

(45 VALUES PER PHOTO)

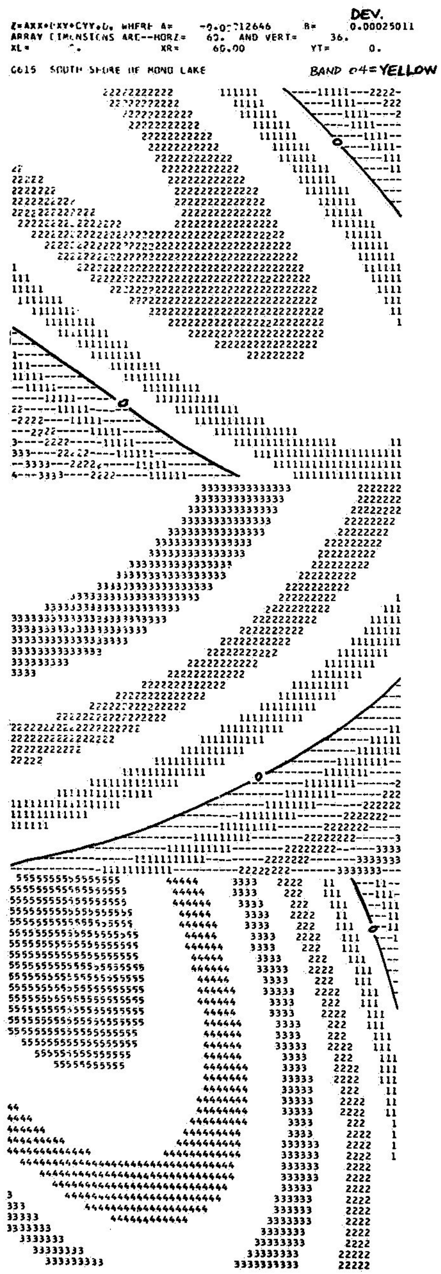

BAND 4

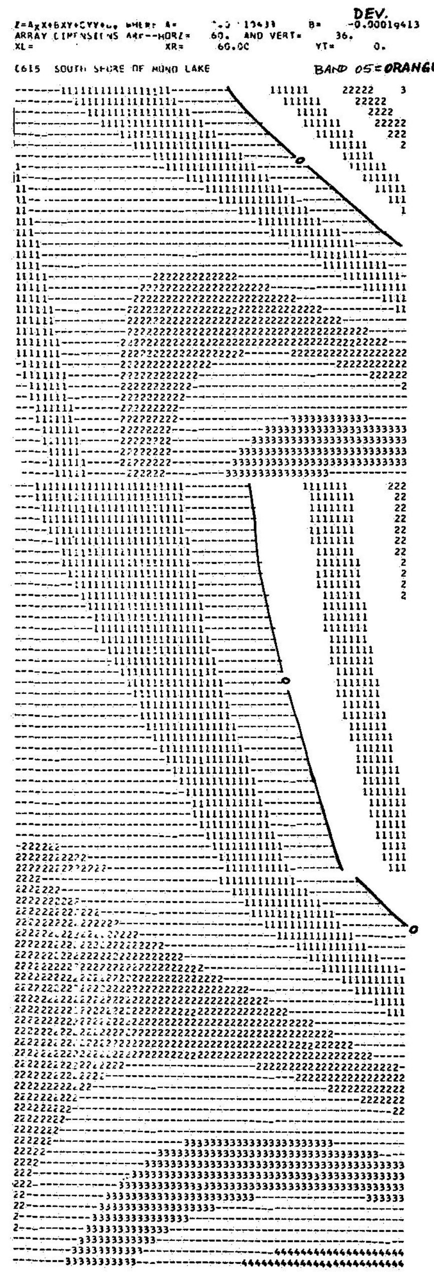

BAND 5

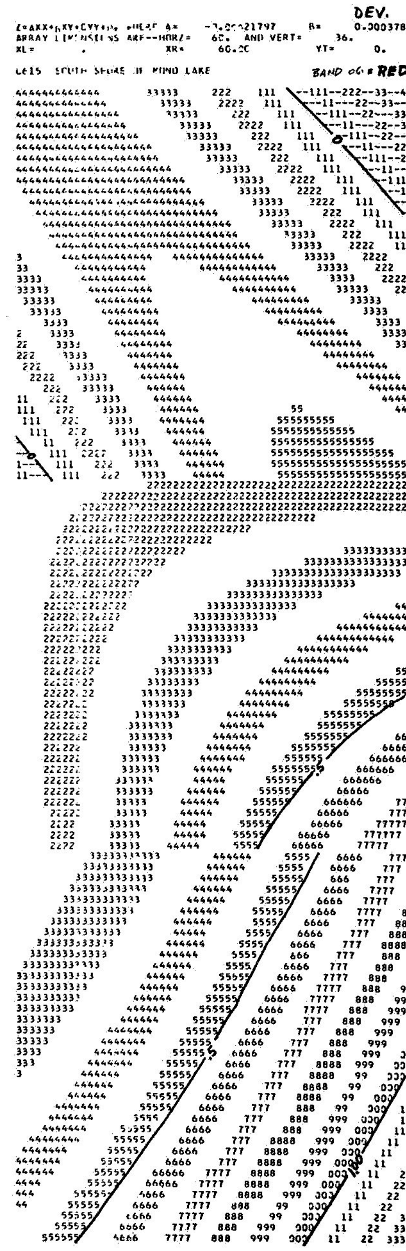

BAND 6

Figure 14

types, then the mean of the value of each of the spectral bands within each type would provide an "ideal" set of numbers for every terrain type. Having made this assumption, we might also assume that the group of values which are "closest" to an unknown spectrum would become the most nearly correct terrain type for this unknown spectrum. One method of comparing the spectrum to be classified with the several possible spectrum is by means of an extension of the Pythagorean theorum into the <u>sixth</u> dimension.* In this case, each dimension is the value of the transmittance of each band. For an example in the <u>second</u> dimension, the distance from an unknown spectrum with transmittance values for each of two bands B1 and B2 can be compared with a mean spectrum for rhyolite, R1 and R2, by computing the distance D between the two. Here, $D^2 = (B1 - R1)^2 + (B2 - R2)^2$ with <u>D</u> being the square-root of the right-hand side of the equation.

The distance thus obtained can be used with a value in a <u>third</u> dimension, and this in turn may be used to find distances in higher dimensions. (This calculation can be done very simply by means of a DO loop in FORTRAN IV, and the minimum distance among several terrain types chosen either by means of an IF statement or the MIN function). The effectiveness of this method in classifying terrain types was not as good as expected, largely because of the extreme variability of many of the band transmission values. If the amount of variation in the spectra being classified

---

*See page 53 of the Appendix for additional information.

is great, then this may cause many of them to be incorrectly identified. A large variation of one band relative to another is the greatest weakness of this system. In order that this variability could be accounted for, statistical methods were resorted to in the last method to be investigated.

3. Statistical Models

The use of statistical methods was first suggested by a computer program which was used in connection with a statistics couse (Geology 205) given by Dr. Paul Switzer in the Spring quarter, 1967, at Stanford. This was a program for Stepwise Discriminant Analysis (BMDO7M) and was written by the UCLA Health Science Computing Facility. The following method requires means and standard deviations fo film transmittances for each of the terrain types to be calculated as they are used in classification. The results of this general program indicated a maximum accuracy, from a choice of three groups, of 80% correct identification for an unknown spectrum obtained from six multiband transparencies. To be more specific a new FORTRAN IV program to produce a classification map was written for this project.

As each of the six bands may be considered a variable and each of the three possible terrain types may be considered a group, the method of multivariate analysis can be used and the resulting classification checked against actual conditions. First, a "perfect" spectrum for each terrain group is decided upon--the means of each group--and is calculated thus:

$$H^R = (h_1^R, h_2^R, \ldots, h_6^R); \; h_i^R = \frac{1}{n_R} \sum_{j=1}^{n} \left(b_{ij}^R\right) \; ; \text{ e.g. } h_1^R = \frac{1}{18} \sum_{j=1}^{18} \left(b_{1j}^R\right) = 0.65167$$

$$H^S = (h_1^S, h_2^S, \ldots, h_6^S);\; h_i = \frac{1}{nS}\sum_{j=1}^{n}\left(b_{ij}^R\right) \;;\; \text{e.g. } h_1^S = \frac{1}{15}\sum_{j=1}^{15}\left(b_{1j}^S\right) = 0.4000$$

$$H^P = (h_1^P, h_2^P, \ldots, h_6^P);\; h_i = \frac{1}{n_P}\sum_{j=1}^{n}\left(b_{ij}^R\right) \;;\; \text{e.g. } h_1^P = \frac{1}{46}\sum_{j=1}^{46}\left(b_{1j}^P\right) = 0.54696$$

where H^R, H^S, H^P are each a set of 6 band means for rhyolite, shadow, or pumice; h_i^R, h_i^S, h_i^P are the means of an individual band i; n_R, n_S, n_P are the number of spectra in each of the three groups; and b_{ij}^R, b_{ij}^S, b_{ij}^P are the relative reflectance values of an individual band in an individual spectrum j.

By using these means as the most probable estimates we may also assume that any variation within an individual band is not completely random, but may be approximated by a Gaussian function of some form. This implies that the three distributions in a given band are each represented by a characteristically shaped normal curve with its peak at the mean of that band. Unknown spectra may then be compared to these ideal spectra and the most probable group decided upon (Fig. 15).

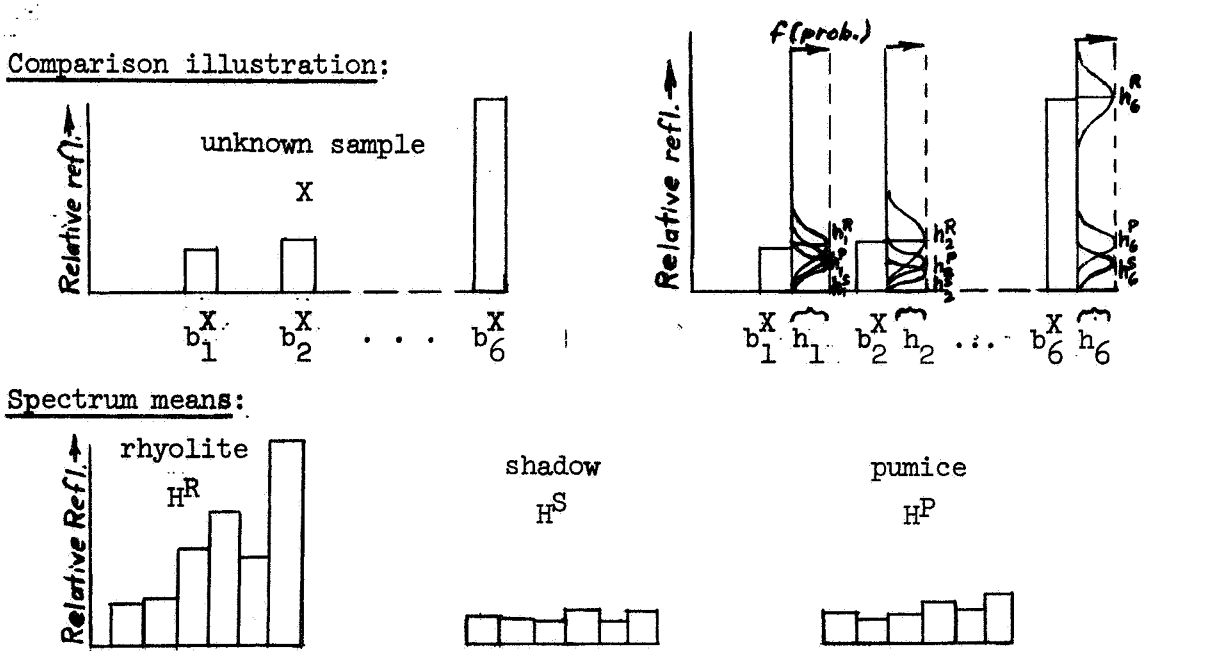

Figure 15

This was done for each known group and for each of the six bands in sequence. Next, the probabilities were totalled and the group with the largest probability was assinged to the unknown spectrum. The value of this probability was computed by dividing the sum of the total probability of the six bands by six and was printed beneath the code name of the group in its proper location relative to the photo.

The three terrain types used were areas of rhyolite obsidian (RHYOLT), rhyolite pumice with little or no sage (PUMICE), and areas of shadow falling on any terrain (SHADOW). The results of this method were about 50% correct using these three groups, however, a fourth group was added which consisted of areas of moderately vegetated pumice (PUMISG), and the original program was modified to consider this group with the others (Fig. 16). The results were more encouraging, with five of the six unknown terrain types in the Crater correctly classified. There were, however, few probability values greater than 0.80, but this was acceptable. Even dark lake water was "correctly" classified as shadow though only having a probability of 0.425.

Other possible terrain types were included in subsequent versions of this new program, but did not show promising results, because those groups had standard deviations (i.e. broad "vague" distribution curves) and were always selected. Another approach involved substituting the values of DEV obtained from a previous program for the values of transmittance. The results of this DEV program were also unsatisfactory, as groups with little variation between bands were confused with each other. This was the case with lake water, which was

MULTIVARIATE CLASSIFICATION OF TERRAIN TYPES NEAR MONO LAKE, CALIFORNIA

DATA FROM SIX VISUAL BANDS OF MULTIBAND PHOTOGRAPHY

0615 SOUTH SHORE OF MONO LAKE

PUMI50	BECH99	BECH99	BECH99	■
PUMI50	PUMI70	PUMI50	BECH99	■
PUMI50	PUMI70	PUMI50	PUMI70	BECH99
PUMI50	PUMI70	PUMI50	PUMI70	BECH05
PUMI50	PUMI70	PUMI50	PUMI70	PUMI70
PUMI50	PUMI70	PUMI50	PUMI70	PUMI50
PUMI50	PUMI70	PUMI50	PUMI70	PUMI50
PUMI50	PUMI70	PUMI50	PUMI70	PUMI50
PUMI50	PUMI70	PUMI50	PUMI70	PUMI50

0615 SOUTH SHORE OF MONO LAKE

PUMISG 0.8256	PUMISG 0.8243	PUMICE 0.7169	PUMISG 0.7020	■ 0.4250
PUMISG 0.7681	PUMICE 0.6896	■ 0.7504	PUMICE 0.6265	■ 0.6554
PUMISG 0.7991	PUMICE 0.8595	PUMICE 0.7001	PUMICE 0.6962	■ 0.6066
PUMISG 0.7646	PUMICE 0.7725	■ 0.7834	PUMICE 0.6286	PUMICE 0.7972
PUMISG 0.8106	PUMICE 0.7405	PUMICE 0.7775	PUMICE 0.7626	PUMISG 0.5704
PUMISG 0.8138	PUMICE 0.7156	PUMICE 0.7844	PUMICE 0.7648	PUMISG 0.6664
PUMISG 0.5934	■ 0.6465	PUMICE 0.7161	PUMICE 0.6859	PUMISG 0.6876
PUMISG 0.6752	■ 0.6930	PUMICE 0.7176	■ 0.8002	PUMISG 0.5989
PUMISG 0.6884	PUMICE 0.8394	■ 0.4382	PUMISG 0.5553	PUMISG 0.4703

0616 NORTH CRATER

PUMI50	PUMI50	PUMI90	PUMI70	PUMI50
RODT99	PUMI50	■	PUMI99	PUMI50
PUMI50	PUMI50	■	■	PUMI50
PUMI50	PUMI50	■	■	PUMI50
PUMI50	PUMI50	■	PUMI90	PUMI70
PUMI50	RODT99	PUMI90	PUMI70	■
PUMI50	PUMI50	PUMI70	PUMI70	■
PUMI50	PUMI50	PUMI70	PUMI70	PUMI50
PUMI50	PUMI50	PUMI70	PUMI70	PUMI50

0616 NORTH CRATER

PUMISG 0.5522	PUMISG 0.6497	■ 0.6054	PUMISG 0.5784	PUMISG 0.5749
PUMISG 0.4818	■ 0.4754	■ 0.5730	■ 0.4790	PUMISG 0.5986
PUMISG 0.7208	■ 0.4265	■ 0.5611	■ 0.4998	■ 0.5374
PUMISG 0.8242	■ 0.5656	PUMISG 0.5995	■ 0.2272	PUMICE 0.6608
PUMISG 0.8145	■ 0.6670	■ 0.4866	■ 0.1338	■ 0.5807
PUMISG 0.8740	PUMICE 0.7527	PUMICE 0.6890	PUMICE 0.8237	PUMISG 0.4535
PUMISG 0.7337	PUMICE 0.7613	■ 0.8363	■ 0.4189	■ 0.4718
PUMISG 0.7263	PUMICE 0.7107	PUMICE 0.6751	■ 0.7535	■ 0.5544
PUMISG 0.7860	PUMISG 0.8107	PUMICE 0.7513	■ 0.6390	PUMISG 0.3214

0617 AREA SOUTH OF NORTH CRATER

PUMI50	PUMI50	PUMI50	PUMI70	PUMI50
RODT99	PUMI50	PUMI50	PUMI50	PUMI50
PUMI50	PUMI50	PUMI50	RODT99	PUMI50
PUMI50	PUMI50	PUMI50	PUMI30	PUMI50
PUMI50	PUMI50	PUMI50	PUMI30	PUMI50
PUMI50	PUMI50	RODT99	PUMI30	RODT99
PUMI50	PUMI50	PUMI70	PUMI30	PUMI50
PUMI50	PUMI50	PUMI70	PUMI30	PUMI50
RODT99	PUMI50	PUMI70	PUMI30	PUMI50

0617 AREA SOUTH OF NORTH CRATER

PUMISG 0.3572	PUMICE 0.6660	PUMICE 0.8501	PUMICE 0.7006	PUMISG 0.6846
PUMISG 0.5792	PUMISG 0.6920	PUMICE 0.6781	PUMICE 0.7528	PUMISG 0.8749
PUMISG 0.6678	PUMISG 0.6653	PUMISG 0.7159	■ 0.4821	PUMISG 0.7159
PUMISG 0.6353	PUMISG 0.6632	PUMISG 0.5963	■ 0.6772	■ 0.6042
PUMISG 0.6026	PUMISG 0.6200	PUMICE 0.6903	■ 0.5255	■ 0.5775
PUMISG 0.8066	PUMICE 0.6137	PUMISG 0.7534	PUMICE 0.6986	■ 0.4101
■ 0.4469	PUMISG 0.5654	PUMICE 0.6459	PUMISG 0.6357	PUMISG 0.5545
PUMISG 0.4491	PUMISG 0.6658	PUMISG 0.6856	■ 0.4473	PUMISG 0.5279
■ 0.3162	PUMISG 0.7279	PUMISG 0.7307	■ 0.5769	PUMISG 0.5668

1 Km

N

TERRAIN TYPES FOUND IN AREA:

RHY099 = RHYOLITE WITH LITTLE OR NO VEGETATION
PUMI99 = PUMICE WITH LITTLE OR NO VEGETATION
PUMI70 = PUMICE WITH SMALL PERCENTAGE OF VEGETATION
PUMI50 = PUMICE AND VEGETATION (SAGE) ABOUT EQUAL
PUMI30 = HEAVILY VEGETATED PUMICE
BECH99 = BEACH DEPOSITS WITH LITTLE OR NO VEGETATION
LAKE99 = LAKE WATER
RODT99 = DIRT ROAD OF PUMICE MATERIAL

TERRAIN TYPES CONSIDERED IN ANALYSIS:

■ RHYOLT = RHYOLITE OBSIDIAN
PUMICE = PUMICE WITH LITTLE OR NO VEGETATION
PUMISG = PUMICE MODERATELY VEGETATED WITH SAGE
SHADOW = SHADED AREAS OF EITHER RHYOLITE OR PUMICE

Figure 16

classified as being pumice. This occurs because the flat, but high reflectance of pumice is compared to the flat, but low reflectance of lake water.

V. CONCLUSIONS

In any attempt at remote sensing data interpretation it must be born in mind that the final classification scheme can only be as reliable as the basic data itself. Any future experiments must be designed so that as many variables as possible can be evaluated. These variables include field reflectance data, major and minor topographic features, soil and vegetation distribution, atmospheric attenuation, aircraft altitude, camera film and filter spectral responses, solar illumination changes with sun angle, and as many other parameters as possible which might influence data obtained during the aircraft overflight.

Assuming all these conditions to be constant for a given time and area, then quantitative multiband data can be obtained by use of recording densitometers, with future data reduction by means of flying-spot densitometers being the next logical step. Secondly, computerized analysis of data provides a rapid means of testing and perfecting methods of classification and discrimination of terrain types, particularly overall geology, from multiband regions under study. It appears that of the three methods of analysis investigated, that statistical multivariate analysis holds the most promise of being an ideal solution for pattern recognition purposes, especially if attempts to classify other areas of similar geology by multiband photography are attempted.

BIBLIOGRAPHY

Colwell, R.N., 1961, Some Practical Applications of Multiband Spectral Reconnaissance: American Scientist, V. 49, No. 1, p. 9-36.

Friedman, J.D., 1966, Geologic Map of the Mono Craters Area, California: NASA Earth Res. Survey Program Technical Letter NASA-12, 11 pp.

Gates, D.M., 1964, Characteristics of Soil and Vegetated Surfaces to Reflected and Emitted Radiation: Proc. of the Third Symposium on Remote Sensing of Environment, Univ. of Michigan, Ann Arbor, Mich., p. 573-600.

Harbaugh, J.W., 1964, A Computer Method for Four-Variable Trend Analysis Illustrated by Study of Oil-Gravity Variations in Southeastern Kansas: Kansas Geol. Survey Bull. 171, 58 pp.

Kistler, R.W., 1966, Structure and Metamorphism in the Mono Craters Quadrangle Sierra Nevada, California: U.S. Geol. Survey Bull. 1221-E, 53 pp.

McCracken, Daniel D., 1966, A Guide to Fortran IV Programming, John Wiley and Sons, Inc.

Molineaux, C.E., 1964 Aerial Reconnaissance of Surface Features with the Multiband Spectral System: Proc. of the Third Symposium on Remote Sensing of Environment, University of Michigan, Ann Arbor, Michigan, p. 399-421.

Moore, J.G., 1947, "The Determination of the Depths and Extinction Coefficients of Shallow Water by Air Photography Using Color Filters": Royal Soc. London, Phil. Trans., Series A, Vol. 240, p. 163-217.

Ray, R.G., and Fischer, W.A., 1960, Quantitative Photography - A Geologic Research Tool: Photogrammetric Engineering , V. 26, No. 1, p. 146-150.

Smith, J.W. and Harbaugh, J.W., 1966, Stratigraphic and Geographic Variation of Shale-oil Specific Gravity from Colorado's Green River Formation: U.S. Bureau of Mines Report of Investigations 6883, p. 5-7.

Switzer, P., 1967, A Statistical Analysis of Spectral Matching in "Field Infrared Analysis of Terrain": Semi-Annual Report, NASA Grant NGR-05-020-115.

Thompson, M.M., Manual of Photogrammetry, 1966, Third Edition, Vol. II. American Society of Photogrammetry, p. 1108.

Toy, H.D. 1966, Anthology on NASA 926 and NASA 927 Aircraft as Applied to Earth Resources Survey Program: NASA Office of Space Science and Applications, p. 152-154.

Watts, H.V., 1966, Reflectance of Rocks and Minerals to Visible and Ultraviolet Radiation: NASA Earth Res. Survey Program Tech. Letter NASA-32, p. 25, 27.

Watts, H.V. and Goldman, H.J., 1967, Visible and Ultraviolet Reflectance and Luminescence from Various Saudi Arabian and Indiana Limestone Rocks: NASA Earth Res. Survey Program Tech Letter NASA-92, p. 13.

APPENDIX

PROGRAM DESCRIPTIONS*

Data Cards:

Each data card used in the following programs contained a coded description of the terrain in the area sampled, the six transmittance values for each of the "spectra", and roll, frame and photograph coordinate numbers. The following examples illustrate this format.

Card column	Description	Example
1-6	Geologic formation	QR = Quaternary rhyolite
7-12	Rock type and percent	RHYØ70 = 70% rhyolite
13-18	Vegetation percent	SAGE25 = 25% sagebrush
19-24	Secondary veg. percent	LICH05 = 5% lichen
25-30	Water type and percent	LAKE99 = entirely lake
31-36	Miscellaneous terrain	RDDT90 = 90% dirt road
37-60	Transmittance values for six visual bands (6F4.2)	Format 6F4.2
61-72	Reserved for IR data	Format 3F4.2
73-76	Exposure number	0615
77-80	X- and Y-coordinates	X = 30, Y = 30

These data cards were then arranged into five groups each having the same X-value and increasing Y-values and a title card placed before each group of 45 spectra. This title card allows a maximum of 72 characters and includes the photograph number and a brief description of the photo area. This is illustrated by the following listing from three digitized photos and one photo profile.

---

*Written for Stanford System IBM 7090 Computer.

0615 SOUTH SHORE OF MONO LAKE

QP	PUMI50SAGE50		65	65	80	100	65	110	0615 1 1
QP	PUMI50SAGE50		55	65	55	80	65	85	0615 1 2
QP	PUMI50SAGE50		60	60	45	75	60	110	0615 1 3
QP	PUMI50SAGE50		65	45	75	75	60	110	0615 1 4
QP	PUMI50SAGE50		70	55	55	80	50	105	0615 1 5
QP	PUMI50SAGE50		70	50	55	85	60	90	0615 1 6
QP	PUMI50SAGE50		80	55	80	50	60	75	0615 1 7
QP	PUMI50SAGE50		80	75	60	65	70	110	0615 1 8
QP	PUMI50SAGE50		75	75	70	85	80	100	0615 1 9
QP	BECH99SAGE01		55	65	60	90	60	85	0615 2 1
QP	PUMI70SAGE30		45	40	30	80	45	70	0615 2 2
QP	PUMI70SAGE30		50	45	45	70	50	85	0615 2 3
QP	PUMI70SAGE30		50	35	40	65	45	80	0615 2 4
QP	PUMI70SAGE30		55	35	40	60	40	85	0615 2 5
QP	PUMI70SAGE30		50	45	40	60	35	60	0615 2 6
QP	PUMI70SAGE30		60	40	40	50	35	55	0615 2 7
QP	PUMI70SAGE30		50	40	35	45	30	60	0615 2 8
QP	PUMI70SAGE30		50	50	45	65	50	70	0615 2 9
QP	BECH99SAGE01		45	55	45	65	50	60	0615 3 1
QP	PUMI50SAGE50		30	35	25	50	35	50	0615 3 2
QP	PUMI50SAGE50		40	40	40	55	45	70	0615 3 3
QP	PUMI50SAGE50		40	35	35	55	35	75	0615 3 4
QP	PUMI50SAGE50		50	40	40	70	45	90	0615 3 5
QP	PUMI50SAGE50		50	35	50	70	40	70	0615 3 6
QP	PUMI50SAGE50		50	45	40	85	35	80	0615 3 7
QP	PUMI50SAGE50		50	50	40	60	40	85	0615 3 8
QP	PUMI50SAGE50		25	30	10	20	20	25	0615 3 9
QP	BECH99SAGE01		60	85	65	100	80	100	0615 4 1
QP	BECH99SAGE01		35	50	35	70	60	70	0615 4 2
QP	PUMI70SAGE30		60	60	30	70	50	70	0615 4 3
QP	PUMI70SAGE30		45	40	35	70	45	120	0615 4 4
QP	PUMI70SAGE30		50	35	35	70	50	80	0615 4 5
QP	PUMI70SAGE30		55	35	40	60	50	90	0615 4 6
QP	PUMI70SAGE30		60	40	45	40	40	85	0615 4 7
QP	PUMI70SAGE60		40	30	25	35	25	55	0615 4 8
QP	PUMI70SAGE30		70	95	70	120	90	110	0615 4 9
QLK		LAKE99	30	30	05	07	27	07	0615 5 1
QLK		LAKE99	30	25	45	05	25	05	0615 5 2
QP	BECH99SAGE01		70	70	75	150	90	130	0615 5 3
QP	BECH05SAGE95		55	45	25	80	45	75	0615 5 4
QP	PUMI70SAGE30		90	70	65	130	60	140	0615 5 5
QP	PUMI50SAGE50		70	50	75	70	55	75	0615 5 6
QP	PUMI50SAGE50		85	55	55	70	60	80	0615 5 7
QP	PUMI50SAGE50		90	75	50	60	60	110	0615 5 8
QP	PUMI50SAGE50		90	85	85	115	80	110	0615 5 9

0616 NORTH CRATER

QP	PUMI50SAGE50		85	70	75	80	50	60	0616	1	1
QP		RDDT99	70	95	110	140	70	110	0616	1	2
QP	PUMI50SAGE50		60	70	55	110	75	90	0616	1	3
QP	PUMI50SAGE50		60	65	50	95	60	90	0616	1	4
QP	PUMI50SAGE50		60	60	55	80	55	90	0616	1	5
QP	PUMI50SAGE50		70	55	60	85	55	105	0616	1	6
QP	PUMI50SAGE50		90	60	50	80	60	95	0616	1	7
QP	PUMI50SAGE50		85	65	55	100	60	80	0616	1	8
QP	PUMI50SAGE50		85	60	60	80	65	90	0616	1	9
QP	PUMI50SAGE50		60	50	60	60	55	50	0616	2	1
QP	PUMI50SAGE50		40	40	100	110	45	50	0616	2	2
QP	PUMI50SAGE50		25	20	15	20	25	20	0616	2	3
QP	PUMI50SAGE50		30	20	17	30	30	30	0616	2	4
QP	PUMI50SAGE50		40	40	35	60	50	60	0616	2	5
QP		RDCT99	50	35	35	70	45	80	0616	2	6
QP	PUMI50SAGE50		55	35	40	60	45	60	0616	2	7
QP	PUMI50SAGE50		55	40	40	50	45	45	0616	2	8
QP	PUMI50SAGE50		75	60	65	70	60	100	0616	2	9
QP	PUMI90SAGE10		60	70	120	100	90	90	0616	3	1
QR	RHY099LICH01		60	85	190	175	110	170	0616	3	2
QR	RHY099LICH01		50	60	90	205	120	150	0616	3	3
QR	RHY099LICH01		40	40	35	95	60	120	0616	3	4
QR	RHY099LICH01		50	80	30	120	60	240	0616	3	5
QP	PUMI90SAGE10		50	40	70	65	60	80	0616	3	6
QP	PUMI70SAGE30		50	30	35	45	35	55	0616	3	7
QP	PUMI70SAGE30		50	40	45	50	40	50	0616	3	8
QP	PUMI70SAGE30		55	40	40	45	40	70	0616	3	9
QP	PUMI70SAGE30		65	70	100	70	80	80	0616	4	1
QP	PUMI90SAGE10		25	25	20	20	25	10	0616	4	2
QR	RHY099LICH01		50	55	100	110	105	150	0616	4	3
QR	RHY099LICH01		75	120	155	310	220	530	0616	4	4
QP	PUMI90SAGE10		15	10	00	00	05	05	0616	4	5
QP	PUMI70SAGE30		45	40	50	70	50	70	0616	4	6
QP	PUMI70SAGE30		30	20	05	15	25	25	0616	4	7
QP	PUMI70SAGE30		40	30	20	35	30	30	0616	4	8
QP	PUMI70SAGE30		55	40	35	35	40	50	0616	4	9
QP	PUMI50SAGE50		70	70	90	100	95	80	0616	5	1
QP	PUMI50SAGE50		60	75	85	100	95	95	0616	5	2
QP	PUMI50SAGE50		65	85	85	150	120	125	0616	5	3
QP	PUMI50SAGE50		45	40	35	60	55	60	0616	5	4
QP	PUMI70SAGE30		80	70	95	140	105	180	0616	5	5
QR	RHY099SAGE01		100	60	75	140	70	195	0616	5	6
QR	RHY099SAGE01		100	70	105	110	85	125	0616	5	7
QP	PUMI50SAGE50		140	100	120	190	85	245	0616	5	8
QP	PUMI50SAGE50		90	60	95	50	200	160	0616	5	9

0617 AREA SOUTH OF NORTH CRATER

QP	PUMI50SAGE50		110	185	90	150	70	110	0617	1	1
QP		RDDT	70	80	105	110	60	80	0617	1	2
QP	PUMI50SAGE50		70	80	55	120	75	110	0617	1	3
QP	PUMI50SAGE50		55	80	60	120	80	110	0617	1	4
QP	PUMI50SAGE50		65	65	70	150	70	170	0617	1	5
QP	PUMI50SAGE50		70	70	70	90	70	100	0617	1	6
QP	PUMI50SAGE50		90	60	100	20	110	175	0617	1	7
QP	PUMI50SAGE50		80	80	90	120	75	140	0617	1	8
QP		RDDT99	140	150	190	280	170	250	0617	1	9
QP	PUMI50SAGE50		50	55	50	110	45	80	0617	2	1
QP	PUMI50SAGE50		60	60	70	145	50	95	0617	2	2
QP	PUMI50SAGE50		60	60	70	160	70	80	0617	2	3
QP	PUMI50SAGE50		50	50	55	130	70	110	0617	2	4
QP	PUMI50SAGE50		55	60	50	130	65	170	0617	2	5
QP	PUMI50SAGE50		60	40	45	130	45	100	0617	2	6
QP	PUMI50SAGE50		60	50	40	130	35	115	0617	2	7
QP	PUMI50SAGE50		65	50	45	130	50	90	0617	2	8
QP	PUMI50SAGE50		65	45	50	100	45	90	0617	2	9
QP	PUMI50SAGE50		55	45	50	80	40	70	0617	3	1
QP	PUMI50SAGE50		50	50	40	95	40	70	0617	3	2
QP	PUMI50SAGE50		50	50	55	110	55	110	0617	3	3
QP	PUMI50SAGE50		50	50	35	115	55	120	0617	3	4
QP	PUMI50SAGE50		55	40	50	90	45	125	0617	3	5
QP		RDSH99	60	50	70	100	55	125	0617	3	6
QP	PUMI70SAGE30		65	40	35	80	40	85	0617	3	7
QP	PUMI70SAGE30		70	70	60	135	55	125	0617	3	8
QP	PUMI70SAGE30		70	50	50	120	55	100	0617	3	9
QP	PUMI70SAGE30		40	40	40	65	40	80	0617	4	1
QP	PUMI50SAGE50		50	50	60	80	50	70	0617	4	2
QP		RDCT99	60	100	135	110	160	355	0617	4	3
QP	PUMI30SAGE70		60	70	70	125	115	125	0617	4	4
QP	PUMI30SAGE70		40	35	30	70	70	100	0617	4	5
QP	PUMI30SAGE70		50	45	40	80	50	115	0617	4	6
QP	PUMI30SAGE70		70	45	60	80	40	150	0617	4	7
QP	PUMI30SAGE70		50	80	110	80	80	140	0617	4	8
QP	PUMI30SAGE70		60	60	55	160	90	225	0617	4	9
QP	PUMI50SAGE50		75	75	55	100	75	125	0617	5	1
QP	PUMI50SAGE50		65	60	60	70	60	95	0617	5	2
QP	PUMI50SAGE50		50	55	50	75	70	95	0617	5	3
QP	PUMI50SAGE50		75	70	70	140	110	190	0617	5	4
QP	PUMI50SAGE50		70	60	70	155	95	240	0617	5	5
		RDDT99	100	105	235	195	140	345	0617	5	6
QP	PUMI50SAGE50		90	65	70	105	75	170	0617	5	7
QP	PUMI50SAGE50		95	70	60	115	55	185	0617	5	8
QP	PUMI50SAGE50		100	65	55	110	45	135	0617	5	9

0616 PRØFILE ØN N-S CENTER LINE

QP	PUMI	SAGE		62	65	95	105	88	90	06163010
QP	PUMI	SAGE		55	57	75	95	61	67	06163011
QR	RHYO			27	18	10	08	10	00	06163012
QR	RHYO			30	19	08	15	15	05	06163013
QR	RHYO			55	58	70	40	55	105	06163014
QR	RHYO			68	83	187	180	110	380	06163015
QR	RHYO			42	40	58	95	55	140	06163016
QR	RHYO			85	102	210	300	172	402	06163017
QR	RHYO			65	78	265	210	120	290	06163018
QR	RHYO			78	85	345	325	224	570	06163019
QR	RHYO			55	60	135	165	158	157	06163020
QR	RHYO			35	30	80	55	61	40	06163021
QR	RHYO			60	66	121	150	107	211	06163022
QR	RHYO			60	57	102	175	90	125	06163023
QR	RHYO			55	42	65	175	100	210	06163024
QR	RHYO			45	38	40	100	63	140	06163025
QR	RHYO			35	23	07	35	30	55	06163026
QR	RHYO			65	60	145	205	183	502	06163027
QR	RHYO			25	20	06	22	25	22	06163028
QR	RHYO			37	21	07	22	22	30	06163029
QR	RHYO			57	77	42	127	60	240	06163030
QR	RHYO			25	10	20	20	23	17	06163031
QP	PUMI	SAGE		50	48	48	95	46	73	06163032
QP	PUMI	SAGE		40	21	37	60	35	47	06163033
QP	PUMI	SAGE		35	16	25	40	25	40	06163034
QP	PUMI	SAGE		65	45	67	87	60	81	06163035
QP	PUMI	SAGE		70	50	60	107	60	88	06163036
QP	PUMI	SAGE		57	34	57	75	50	87	06163037
QP	PUMI	SAGE		60	30	30	60	40	48	06163038
QP	PUMI	SAGE		55	28	35	45	35	72	06163039
QP	PUMI	SAGE		55	31	33	45	35	50	06163040
QP	PUMI	SAGE		55	32	32	50	36	42	06163041
QP	PUMI	SAGE		53	36	45	60	41	63	06163042
QP	PUMI	SAGE		54	36	41	55	38	50	06163043
QP	PUMI	SAGE		55	38	45	55	40	50	06163044
QP	PUMI	SAGE		57	40	43	55	40	50	06163045
QP	PUMI	SAGE		57	35	48	55	48	62	06163046
ROADDT			RDDT	87	86	95	85	80	105	06163047
ROADDT			RDDT	75	60	43	57	50	90	06163048
QP	PUMI	SAGE		60	43	56	65	43	64	06163049
QP	PUMI	SAGE		60	40	40	50	40	70	06163050

Conversion of Data to "Map" Form

In order for some of the following trend surface programs to work in a less complex manner, the original data was "rearranged" and punched on cards. This was accomplished by the following program, which inputs the title card and profile-type data on 45 cards and outputs six sets of band transmittances and the appropriate title card. In essence, this provides six sets of numbers for the individual wavelengths and arranges them from Band 1 to Band 6. Also the format for each card changes from 36X, 6F4.2 to 5F10.2; or from a spectrum to a line of five equal Y-values.

This data rearrangement program is shown in the following listing, along with a listing of the output.

```
$JOB  S060   IBJOB 2      800    BALLEW   GARY       233    BANDPASS MAPS
$IBJOB
$IBFTC MAIN    NODECK
C    ACTUAL BAND-PASS MAPS
      DIMENSION TITLE(12), B(5,9,6)
   99 WRITE(6,98)
   98 FORMAT(1H1,1H )
      READ(5,1) (TITLE(K),K=1,12)
    1 FORMAT (12A6)
      READ(5,3)(((B(L,J,I), I=1,6), J=1,9),L=1,5)
    3 FORMAT(36X,6F4.2)
      DO 100 I=1,6
      WRITE(6,10) (TITLE(K),K=1,12),I
   10 FORMAT(1HP,12A6, 4HBAND,I3/ )
      DO 100 J=1,9
      WRITE(6,4)(B(L,J,I),L=1,5)
    4 FORMAT(1HP,5F10.2/   )
  100 CONTINUE
      GO TU 99
      RETURN
      END
?32                  PRECEDES B5000 AND IBJOB DATA CARDS
```

0615 SOUTH SHORE OF MONO LAKE BAND 1

0.65	0.55	0.45	0.60	0.30
0.55	0.45	0.30	0.35	0.30
0.60	0.50	0.40	0.60	0.70
0.65	0.50	0.40	0.45	0.55
0.70	0.55	0.50	0.50	0.90
0.70	0.50	0.50	0.55	0.70
0.80	0.60	0.50	0.60	0.85
0.80	0.50	0.50	0.40	0.90
0.75	0.50	0.25	0.70	0.90

0615 SOUTH SHORE OF MONO LAKE BAND 2

0.65	0.65	0.55	0.85	0.30
0.65	0.40	0.35	0.50	0.25
0.60	0.45	0.40	0.60	0.70
0.45	0.35	0.35	0.40	0.45
0.55	0.35	0.40	0.35	0.70
0.50	0.45	0.35	0.35	0.50
0.55	0.40	0.45	0.40	0.55
0.75	0.40	0.50	0.30	0.75
0.75	0.50	0.30	0.95	0.85

0615 SOUTH SHORE OF MONO LAKE BAND 3

0.80	0.60	0.45	0.65	0.05
0.55	0.30	0.25	0.35	0.45
0.45	0.45	0.40	0.30	0.75
0.75	0.40	0.35	0.35	0.25
0.55	0.40	0.40	0.35	0.65
0.55	0.40	0.50	0.40	0.75
0.80	0.40	0.40	0.45	0.55
0.60	0.35	0.40	0.25	0.50
0.70	0.45	0.10	0.70	0.85

0615 SOUTH SHORE OF MONO LAKE BAND 4

1.00	0.90	0.65	1.00	0.07
0.80	0.80	0.50	0.70	0.05
0.75	0.70	0.55	0.70	1.50
0.75	0.65	0.55	0.70	0.80
0.80	0.60	0.70	0.70	1.30
0.85	0.60	0.70	0.60	0.70
0.50	0.50	0.85	0.40	0.70
0.65	0.45	0.60	0.35	0.60
0.85	0.65	0.20	1.20	1.15

0615 SOUTH SHORE OF MONO LAKE BAND 5

0.65	0.60	0.50	0.80	0.27
0.65	0.45	0.35	0.60	0.25
0.60	0.50	0.45	0.50	0.90
0.60	0.45	0.35	0.45	0.45
0.50	0.40	0.45	0.50	0.60
0.60	0.35	0.40	0.50	0.55
0.60	0.35	0.35	0.40	0.60
0.70	0.30	0.40	0.25	0.60
0.80	0.50	0.20	0.90	0.80

0615 SOUTH SHORE OF MONO LAKE BAND 6

1.10	0.85	0.60	1.00	0.07
0.85	0.70	0.50	0.70	0.05
1.10	0.85	0.70	0.70	1.30
1.10	0.80	0.75	1.20	0.75
1.05	0.85	0.90	0.80	1.40
0.90	0.60	0.70	0.90	0.75
0.75	0.55	0.80	0.85	0.80
1.10	0.60	0.85	0.55	1.10
1.00	0.70	0.25	1.10	1.10

0616 NORTH CRATER BAND 1

0.85	0.60	0.60	0.65	0.70
0.70	0.40	0.60	0.25	0.60
0.60	0.25	0.50	0.50	0.65
0.60	0.30	0.40	0.75	0.45
0.60	0.40	0.50	0.15	0.80
0.70	0.50	0.50	0.45	1.00
0.90	0.55	0.50	0.30	1.00
0.85	0.55	0.50	0.40	1.40
0.85	0.75	0.55	0.55	0.90

0616 NORTH CRATER BAND 2

0.70	0.50	0.70	0.70	0.70
0.95	0.40	0.85	0.25	0.75
0.70	0.20	0.60	0.55	0.85
0.65	0.20	0.40	1.20	0.40
0.60	0.40	0.80	0.10	0.70
0.55	0.35	0.40	0.40	0.60
0.60	0.35	0.30	0.20	0.70
0.65	0.40	0.40	0.30	1.00
0.60	0.60	0.40	0.40	0.60

0616 NORTH CRATER BAND 3

0.75	0.60	1.20	1.00	0.90
1.10	1.00	1.90	0.20	0.85
0.55	0.15	0.90	1.00	0.85
0.50	0.17	0.35	1.55	0.35
0.55	0.35	0.30	0.	0.95
0.60	0.35	0.70	0.50	0.75
0.50	0.40	0.35	0.05	1.05
0.55	0.40	0.45	0.20	1.20
0.60	0.65	0.40	0.35	0.95

0616 NORTH CRATER BAND 4

0.80	0.60	1.00	0.70	1.00
1.40	1.10	1.75	0.20	1.00
1.10	0.20	2.05	1.10	1.50
0.95	0.30	0.95	3.10	0.60
0.80	0.60	1.20	0.	1.40
0.85	0.70	0.65	0.70	1.40
0.80	0.60	0.45	0.15	1.10
1.00	0.50	0.50	0.35	1.90
0.80	0.70	0.45	0.35	0.50

0616 NORTH CRATER BAND 5

0.50	0.55	0.90	0.80	0.95
0.70	0.45	1.10	0.25	0.95
0.75	0.25	1.20	1.05	1.20
0.60	0.30	0.60	2.20	0.55
0.55	0.50	0.60	0.05	1.05
0.55	0.45	0.60	0.50	0.70
0.60	0.45	0.35	0.25	0.85
0.60	0.45	0.40	0.30	0.85
0.65	0.60	0.40	0.40	2.00

0616 NORTH CRATER BAND 6

0.60	0.50	0.90	0.80	0.80
1.10	0.50	1.70	0.10	0.95
0.90	0.20	1.50	1.50	1.25
0.90	0.30	1.20	5.30	0.60
0.90	0.60	2.40	0.05	1.80
1.05	0.80	0.80	0.70	1.95
0.95	0.60	0.55	0.25	1.25
0.80	0.45	0.50	0.30	2.45
0.90	1.00	0.70	0.50	1.60

0617 AREA SOUTH OF NORTH CRATER BAND 1

1.10	0.50	0.55	0.40	0.75
0.70	0.60	0.50	0.50	0.65
0.70	0.60	0.50	0.60	0.50
0.55	0.50	0.50	0.60	0.75
0.65	0.55	0.55	0.40	0.70
0.70	0.60	0.60	0.50	1.00
0.90	0.60	0.65	0.70	0.90
0.80	0.65	0.70	0.50	0.95
1.40	0.65	0.70	0.60	1.00

0617 AREA SOUTH OF NORTH CRATER BAND 2

1.85	0.55	0.45	0.40	0.75
0.80	0.60	0.50	0.50	0.60
0.80	0.60	0.50	1.00	0.55
0.80	0.50	0.50	0.70	0.70
0.65	0.60	0.40	0.35	0.60
0.70	0.40	0.50	0.45	1.05
0.60	0.50	0.40	0.45	0.65
0.80	0.50	0.70	0.80	0.70
1.50	0.45	0.50	0.60	0.65

0617 AREA SOUTH OF NORTH CRATER BAND 3

0.90	0.50	0.50	0.40	0.55
1.05	0.70	0.40	0.60	0.60
0.55	0.70	0.55	1.35	0.50
0.60	0.55	0.35	0.70	0.70
0.70	0.50	0.50	0.30	0.70
0.70	0.45	0.70	0.40	2.35
1.00	0.40	0.35	0.60	0.70
0.90	0.45	0.60	1.10	0.60
1.90	0.50	0.50	0.55	0.55

0617 AREA SOUTH OF NORTH CRATER BAND 4

1.50	1.10	0.80	0.65	1.00
1.10	1.45	0.95	0.80	0.70
1.20	1.60	1.10	1.10	0.75
1.20	1.30	1.15	1.25	1.40
1.50	1.30	0.90	0.70	1.55
0.90	1.30	1.00	0.80	1.95
0.20	1.30	0.80	0.80	1.05
1.20	1.30	1.35	0.80	1.15
2.80	1.00	1.20	1.60	1.10

0617 AREA SOUTH OF NORTH CRATER BAND 5

0.70	0.45	0.40	0.40	0.75
0.60	0.50	0.40	0.50	0.60
0.75	0.70	0.55	1.60	0.70
0.80	0.70	0.55	1.15	1.10
0.70	0.65	0.45	0.70	0.95
0.70	0.45	0.55	0.50	1.40
1.10	0.35	0.40	0.40	0.75
0.75	0.50	0.55	0.80	0.55
1.70	0.45	0.55	0.90	0.45

0617 AREA SOUTH OF NORTH CRATER BAND 6

1.10	0.80	0.70	0.80	1.25
0.80	0.95	0.70	0.70	0.95
1.10	0.80	1.10	3.55	0.95
1.10	1.10	1.20	1.25	1.90
1.70	1.70	1.25	1.00	2.40
1.00	1.00	1.25	1.15	3.45
1.75	1.15	0.85	1.50	1.70
1.40	0.90	1.25	1.40	1.85
2.50	0.90	1.00	2.25	1.35

Second-Degree Trend Surface

This program provides a method of obtaining a trend surface of each of the colors or bands used in this analysis. This is accomplished by means of a trend surface contour plotting program which has been spliced into another program which solves for the coefficients of the second-order equation. The input for this consists of the six sets of the 45 values of transmittance obtained from each photo and the corresponding title cards. The format of each card is the 5F10.2 format previously described. In addition, the first data card must contain the parameters of the plotted trend surface dimensions.

These output parameters include the horizontal dimension HORZ, vertical dimension VERT, both in terms of lines and spaces; the left, right, top, and bottom dimensions XL, XR, YT, and YB, respectively; the reference contour REF; and the contour interval CON. The output consists of a pattern of alternating blanks and numbers from zero to one for positive numbers, and alternating minus signs and numbers for negative numbers. For best results, the contour interval should be half that of the expected contour interval if whole numbers are used.

The equation used is $Z = AX^2 + BXY + CY^2 + D$, where Z is the transmittance of the trend surface at coordinates X and Y in millimeters from the upper left-hand corner of the photograph, and A, B, C and D are the coefficients which are determined by the SOLVEX subroutine of the program. This subroutine essentially solves the 4 by 4 matrix generated by the least-squared method employed here. This sub-routine may be obtained from the computation center's library of programs under the name SOLVE, program number one, which can solve up to 20 by 20 matrices.

```
$IBJOB         MAP
$IBFTC MAIN
C CONTOUR FROM CARDS IN COORDINATE FORMAT USING SOLVEX
      INTEGER PLUS,MINU,CV
      DIMENSION W(   60),CV(   60),PLUS(   36),MINU(   36),
     1           AA(4,4),BB(4),COEF(4),X(45,3) ,Z(9,5), TITLE(12)
      DATA(PLUS(I),I=1,20)/1H ,1H1,1H ,1H2,1H ,1H3,1H ,1H4,1H ,1H5,1H ,1
     1H6,1H ,1H7,1H ,1H8,1H ,1H9,1H ,1H0/,(MINU(I),I=1,20)/1H-,1H1,1H-,1
     2H2,1H-,1H3,1H-,1H4,1H-,1H5,1H-,1H6,1H-,1H7, 1H-,1H8,1H-,1H9,1H-,1H
     30/
  101 READ(5,99)         HORZ,VERT,XL,XR,YT,YB,REF,CON
   99 FORMAT  (28X,F3.0,F5.0,6F7,2)
  200 READ(5,7) (TITLE(K),K=1,12)
    7 FORMAT(12A6)
      READ(5,8) ((Z(I,J),J=1,5),I=1,9)
    8 FORMAT(5F10.3)
      X4=0.0
      X3Y=0.0
      X2Y2=0.0
      XY3=0.0
      Y4=0.0
      XY=0.0
      Y2=0.0
      X2=0.0
      ZX2=0.0
      ZXY=0.0
      ZY2=0.0
      Z=0.0
      N=0
      X(I,2)=5.0
      DO 100 L=1,9
      X(I,2)=X(I,2) +5.0
      X(I,1)=0.0
      DO 100 M=1,5
      X(I,1)=X(I,1) +10.0
      X(I,3)=Z(L,M)
      X4=X4+X(I,1)*X(I,1)*X(I,1)*X(I,1)
      X3Y=X3Y+X(I,1)*X(I,1)*X(I,1)*X(I,2)
      X2Y2=X2Y2+X(I,1)*X(I,1)*X(I,2)*X(I,2)
      XY3=XY3+X(I,1)*X(I,2)*X(I,2)*X(I,2)
      Y4=Y4+X(I,2)*X(I,2)*X(I,2)*X(I,2)
      XY=XY+X(I,1)*X(I,2)
      Y2=Y2+X(I,2)*X(I,2)
      X2=X2+X(I,1)*X(I,1)
      ZX2=ZX2+X(I,3)*X(I,1)*X(I,1)
      ZXY=ZXY+X(I,3)*X(I,1)*X(I,2)
      ZY2=ZY2+X(I,3)*X(I,2)*X(I,2)
      Z=Z+X(I,3)
      N=N+1
  100 CONTINUE
      RN=N
       AA(1,1)=X4
       AA(1,2)=XY3
       AA(1,3)=X2Y2
       AA(1,4)=X2
```

```
      AA(2,1)=X3Y
      AA(2,2)=X2Y2
      AA(2,3)=XY3
      AA(2,4)=XY
      AA(3,1)=X2Y2
      AA(3,2)=XY3
      AA(3,3)=Y4
      AA(3,4)=Y2
      AA(4,1)=X2
      AA(4,2)=XY
      AA(4,3)=Y2
      AA(4,4)=RN
      BB(1)=ZX2
      BB(2)=ZXY
      BB(3)=ZY2
      BB(4)=Z
      CALL SOLVE (4, AA,BB,1,0,0,10,COEF,IT)
      A=COEF(1)
      B=COEF(2)
      C=COEF(3)
      D=COEF(4)
      WRITE(6,98)A,B,C,D
   98 FORMAT(1H1,25HZ=AXX+BXY+CYY+D, WHERE A=, F15.8,5X,2HB=,F15.8,5X,
     12HC=,F15.8, 5X, 2HD=,F15.8 )
      WRITE(6,97)HORZ,VERT
   97 FORMAT(1H ,27HARRAY DIMENSIONS ARE--HORZ=, F6.0,11H  AND VERT=,F8.
     10)
      WRITE(6,96)XL,XR,YT,YB,REF,CON
   96 FORMAT(1H ,3HXL=,F10.2,10X,3HXR=,F10.2,10X,3HYT=,F10.2,10X,3HYB=,
     1F10.2,10X,4HREF=,F10.2,10X,4HCON=,F10.2//)
      WRITE(6,5) (TITLE(K),K=1,12)
    5 FORMAT(1H ,12A6//)
      DX=(XR-XL)/HORZ
      DY=(YB-YT)/VERT
      C1=(A*XL*XL)+(B*XL*YT)+(C*YT*YT)+D
      C2=(2.*A*XL*DX)+(B*YT*DX)
      C3=A*DX*DX
      C4=(B*XL*DY)+(2.*C*YT*DY)
      C5=C*DY*DY
      C6=B*DX*DY
      IHORZ=HORZ
      IVERT=VERT
      DO 1 I=1,IVERT
      RI=I
      C7=C1+(RI*C4)+(RI*RI*C5)
      C8=(C6*RI)+C2
      DO 2 J=1,IHORZ
      RJ=J
      W(J)=C7+(C8*RJ)+(C3*RJ*RJ)
      IF(W(J).LT.REF) GO TO 3
      XX=(W(J)-REF)/CON
      IX=XX
      IA=MOD(IX,20)
      CV(J)=PLUS(IA+1)
      GO TO 2
```

```
    3 YY=(REF-W(J))/CON
      IY=YY
      IB=MOD(IY,20)
      CV(J)= MINU(IB+1)
    2 CONTINUE
      WRITE(6, 95)(CV(K),K=1,IHORZ)
   95 FORMAT(1HT,132A1)
    1 CONTINUE
      GO TO 200
  102 RETURN
      END
$IBFTC SOLVEX

CSOLVE   LINEAR EQUATION SOLVER WITH ITERATIVE IMPROVEMENT    VERSION IV
      SUBROUTINE SOLVE(NN,A,B,IN,EPS,ITMAX,X,IT)
C     SOLVES AX=B WHERE A IS NXN MATRIX AND B IS NX1 VECTOR
C     IN=
C          1 FOR FIRST ENTRY
C          2 FOR SUBSEQUENT ENTRIES WITH NEW B
C          3 TO RESTORE A AND B
C     EPS AND ITMAX ARE PARAMETERS IN THE ITERATION
C     IT=
C          -1 IF A IS SINGULAR
C          0 IF NOT CONVERGENT
C          NUMBER OF ITERATIONS IF CONVERGENT
C     CALLS MAP SUBROUTINES ILOG2,DOT,SDOT AND DAD
C
C     TO MODIFY DIMENSIONS, CHANGE THE NEXT 3 (NOT 2 BUT 3) CARDS.
      DIMENSION A( 4, 4),B( 4),X( 4),AA( 4, 4),DX( 4),R( 4),
     *          Z( 4),RM( 4),IRP( 4)
      MA= 4
C     MA MUST = DECLARED DIMENSION OF SYSTEM
      EQUIVALENCE(R,DX)
      GO TO (1000,2000,3000),IN
 1000 N=NN
      NM1=N-1
      NP1=N+1
C
C     EQUILIBRATION
C
      DO 510 I=1,N
          KTOP=ILOG2(A(I,1))
          DO 503 J=2,N
  503     KTOP=MAX0(KTOP,ILOG2(A(I,J)))
          RM(I)=2.0**(-KTOP)
          DO 509 J=1,N
  509     A(I,J)=A(I,J)*RM(I)
  510 CONTINUE
C
C     SAVE EQUILIBRATED DATA
C
      DO 548 I=1,N
      DO 548 J=1,N
  548 AA(I,J)=A(I,J)
C
```

```
C     GAUSSIAN ELIMINATION WITH PARTIAL PIVOTING                        SLV4043
C                                                                       SLV4044
      DO 99 M=1,NM1                                                     SLV4045
          TOP=ABS (A(M,M))                                              SLV4046
          IMAX=M                                                        SLV4047
          DO 12 I=M,N                                                   SLV4048
              IF(TOP-ABS (A(I,M)))10,12,12                              SLV4049
   10         TOP=ABS (A(I,M))                                          SLV4050
              IMAX=I                                                    SLV4051
   12     CONTINUE                                                      SLV4052
          IF(TOP)14,13,14                                               SLV4053
   13     IT=-1                                                         SLV4054
C         *SINGULAR*                                                    SLV4055
          RETURN                                                        SLV4056
   14     IRP(M)=IMAX                                                   SLV4057
   23     IF(IMAX-M)29,29,24                                            SLV4058
   24     DO 25 J=1,N                                                   SLV4059
              TEMP=A(M,J)                                               SLV4060
              A(M,J)=A(IMAX,J)                                          SLV4061
   25         A(IMAX,J)=TEMP                                            SLV4062
   29     MP1=M+1                                                       SLV4063
          DO 33 I=MP1,N                                                 SLV4064
              EM=A(I,M)/A(M,M)                                          SLV4065
              A(I,M)=EM                                                 SLV4066
              IF(EM)31,33,31                                            SLV4067
   31         DO 32 J=MP1,N                                             SLV4068
   32         A(I,J)=A(I,J)-A(M,J)*EM                                   SLV4069
   33     CONTINUE                                                      SLV4070
   99 CONTINUE                                                          SLV4071
      IRP(N)=N                                                          SLV4072
      IF (A(N,N))120,113,120                                            SLV4073
  113 IT=-1                                                             SLV4074
      RETURN                                                            SLV4075
  120 CONTINUE                                                          SLV4076
C     STORAGE FOR A NOW CONTAINS TRIANGULAR L AND U SO THAT (L+I)*U=A   SLV4077
C                                                                       SLV4078
C     DUPLICATE INTERCHANGES IN DATA                                    SLV4079
C                                                                       SLV4080
      DO 229 I=1,N                                                      SLV4081
          IP=IRP(I)                                                     SLV4082
          IF(I-IP)221,229,221                                           SLV4083
  221     DO 222 J=1,N                                                  SLV4084
              TEMP=AA(I,J)                                              SLV4085
              AA(I,J)=AA(IP,J)                                          SLV4086
  222         AA(IP,J)=TEMP                                             SLV4087
  229 CONTINUE                                                          SLV4088
C                                                                       SLV4089
C     PROCESS RIGHT HAND SIDE                                           SLV4090
C                                                                       SLV4091
 2000 CONTINUE                                                          SLV4092
      DO 601 I=1,N                                                      SLV4093
  601     B(I)=B(I)*RM(I)                                               SLV4094
      DO 609 I=1,NM1                                                    SLV4095
          IP=IRP(I)                                                     SLV4096
          TEMP=B(I)                                                     SLV4097
```

```
          B(I)=B(IP)
          B(IP)=TEMP
  609 CONTINUE
C
C     SOLVE FOR FIRST APPROXIMATION TO X
C
  199 DO 200 I=1,N
  200 Z(I)=-SDOT(I-1,A(I,1),MA,Z(1),1,-B(I))
      DO 201 K=1,N
      I=NP1-K
  201 X(I)=-SDOT(N-I,A(I,I+1),MA,X(I+1),1,-Z(I))/A(I,I)
C
C     ITERATIVE IMPROVEMENT
C
      IF(ITMAX)370,370,300
  300 TOP=0.0
      DO 303 I=1,N
  303 TOP=AMAX1(TOP,ABS(X(I)))
      EPSX=EPS*TOP
      DO 369 IT=1,ITMAX
C         FIND RESIDUALS
          DO 319 I=1,N
  319     R(I)=-DOT(N,AA(I,1),MA,X(1),1,-B(I))
C         FIND INCREMENT
          DO 329 I=1,N
  329     Z(I)=-SDOT(I-1,A(I,1),MA,Z(1),1,-R(I))
          DO 339 K=1,N
          I=NP1-K
  339     DX(I)=-SDOT(N-I,A(I,I+1),MA,DX(I+1),1,-Z(I))/A(I,I)
C         INCREMENT AND TEST CONVERGENCE
          TOP=0.0
          DO 342 I=1,N
              TEMP=X(I)
              X(I)=DAD(X(I),DX(I))
              DELX=ABS (X(I)-TEMP)
              TOP=AMAX1(TOP,DELX)
  342     CONTINUE
          IF(TOP-EPSX)381,381,369
  369 CONTINUE
  370 IT=0
  381 RETURN
C
C     RESTORE A AND B
C
 3000 CONTINUE
      DO 709 K=1,N
          I=NP1-K
          IP=IRP(I)
          IF(I-IP)701,709,701
  701     TEMP=B(I)
          B(I)=B(IP)
          B(IP)=TEMP
          DO 702 J=1,N
              TEMP=AA(I,J)
              AA(I,J)=AA(IP,J)
```

```
  702            AA(IP,J)=TEMP                                          SLV4153
  709 CONTINUE                                                          SLV4154
      DO 729 I=1,N                                                      SLV4155
          B(I)=B(I)/RM(I)                                               SLV4156
          DO 729 J=1,N                                                  SLV4157
          A(I,J)=AA(I,J)/RM(I)                                          SLV4158
  729 CONTINUE                                                          SLV4159
      RETURN                                                            SLV4160
      END                                                               SLV4161
$IBMAP DOT       84                                                     DOT4000
*   DOT AND FRIENDS      ROUTINES FOR USE WITH SOLVE                    DOT4001
        ENTRY    DOT (N,A(1),MA,B(1),MB,C)   DOUBLE INNER PRODUCT       DOT4002
        ENTRY    SDOT (N,A(1),MA,B(1),MB,C)  INNER PRODUCT              DOT4003
        ENTRY    ILOG2 (A)    FLOATING POINT EXPONENT                   DOT4004
        ENTRY    DAD (A,B)    ADD WITH ROUND                            DOT4005
*                                                                       DOT4006
SNAD    MACRO    M      STORE NEGATIVE OF ADDRESS IN DECREMENT          DOT4007
        SUB      =O100000         COMPLEMENT IF POSITIVE                DOT4008
        ALS      18                                                     DOT4009
        STD      M                                                      DOT4010
        ENDM     SNAD                                                   DOT4011
*                                                                       DOT4012
DOT     SAVE     1,2,4                                                  DOT4013
        STZ      S                                                      DOT4014
        STZ      S+1                                                    DOT4015
        CLA*     8,4              C                                     DOT4016
        LDQ      C+1                                                    DOT4017
        STO      C                                                      DOT4018
        CLA*     3,4              N                                     DOT4019
        TZE      NONE             SKIP LOOP IF N = 0                    DOT4020
        STO      N                                                      DOT4021
        CLA      4,4              BASE ADDRESS OF A                     DOT4022
        PAC      ,1               X1=-(BASE OF A)                       DOT4023
        CLA*     5,4              MA                                    DOT4024
        SNAD     MA                                                     DOT4025
        CLA      6,4              BASE ADDRESS OF B                     DOT4026
        PAC      ,2               X2=-(BASE OF B)                       DOT4027
        CLA*     7,4              MB                                    DOT4028
        SNAD     MB                                                     DOT4029
        LXA      N,4              X4=N                                  DOT4030
 LOOP   LDQ      0,1              A(I)                                  DOT4031
        FMP      0,2              B(I)                                  DOT4032
        DFAD     S                                                      DOT4033
        DST      S                                                      DOT4034
 MA     TXI      *+1,1,**         (X1)=(X1)+MA                          DOT4035
 MB     TXI      *+1,2,**         (X2)=(X2)+MB                          DOT4036
        TIX      LOOP,4,1         END OF MAIN LOOP                      DOT4037
NONE    DFAD     C                                                      DOT40380
        FRN                                                             DOT40390
        RETURN   DOT                                                    DOT40400
*                                                                       DOT40410
SDOT    SAVE     1,2,4                                                  DOT40420
        STZ      S                                                      DOT40430
        CLA*     8,4                                                    DOT40440
        STO      C                                                      DOT40450
```

```
         CLA*     3,4
         TZE      SNONE
         STO      N
         CLA      4,4
         PAC      ,1
         CLA*     5,4
         SNAU     SMA
         CLA      6,4
         PAC      ,2
         CLA*     7,4
         SNAU     SMB
         LXA      N,4
SLOOP    LDQ      0,1
         FMP      0,2
         FAD      S
         STO      S
SMA      TXI      *+1,1,**
SMB      TXI      *+1,2,**
         TIX      SLOOP,4,1
SNONE    FAD      C
         RETURN   SDOT
*
ILOG2    CAL*     3,4
         ANA      =0377000000000
         SUB      =0200000000000
         ARS      27
         TRA      1,4
*
DAD      CLA*     3,4
         FAD*     4,4
         FRN
         TRA      1,4
*
         EVEN
C        PZE
         PZE
S        PZE
         PZE
N        PZE
         END
```

Six-Dimensional Classification of Spectra

This program essentially computes the distance from an unknown spectrum of six bands to the means of three general terrain types--all this in theoretically six dimensions of transmittance. The group which is closest to the unknown spectrum is then assumed to be the most likely choice and is printed in the proper location. This distance is known as the Mahalanobis or M-distance and is an extension of the Pythagorean theorem. In this program the distance in two dimensions is computed and this distance used to compute the third dimension, and higher dimensions in sequence up to six.

The means of the bands for each group are input using a DATA statement, as are the names of these groups. The spectra cards are used in the format first presented for the remaining input, while the output consists of the six-letter code name of the group selected for each spectrum and its distance in percent transmittance to the unknown spectrum. If the amount of variation in the spectra being classified is great, then this may cause many of them to be incorrectly identified. A large variation of one band relative to another is the greatest weakness of this system.

```
$JOB  R563  IBJOB  2    800   BALLEW, GARY      233   6-D GEOMAP
$IBJOB
$IBFTC MAIN
C MULTIDIMENSIONAL CLASSIFICATION OF MULTIBAND SPECTRA
      DIMENSION TITLE(12), SYMBOL(60),XNAME(  5), BAND(5,9,6),
     1              AMEAN(3,6),   ANAME(3), RMIN(5), D2(3)
      DATA   (ANAME(NG),     NG=1,3)/ 6HRHYOLT, 6HPUMICE, 6HSHADOW/
      DATA  ((AMEAN(NG, I), I=1,6),NG=1,3) / 0.65167, 0.71111,  1.33167,
     1 1.82056, 1.19667,  2.64833,
     2  0.54696, 0.43913, 0.47870, 0.68239, 0.48196, 0.74174,
     3  0.40000, 0.27467,  0.31400, 0.45133, 0.35533, 0.52067/
      DATA (SYMBOL(L)  ,L=1,60) / 60*1H./
 1000 READ(5,1)(TITLE(K),K=1,12)
    1 FORMAT(12A6)
      WRITE(6,2) (TITLE(K), K=1,12)
    2 FORMAT(1H1,12A6)
      WRITE(6,401)(SYMBOL(L),L=1,60)
      WRITE(6,303)
      WRITE(6,303)
      READ(5,3) (((BAND(NX,NY,I),I= 1,6), NY=1,9) ,NX=1,5)
    3 FORMAT (36X,6F4.2)
      DO 400 NY=1,9
      DO 300 NX=1,5
      RMIN(NX)=0.0
      DO 200 NG=1,3
      D2(NG) = 0.0
      DO 100 I=1,6
      D2(NG)        =D2(NG)       + (AMEAN(NG,I) -BAND(NX,NY,I)) *
     1   (AMEAN(NG,I)  - BAND(NX,NY,I))
  100 CONTINUE
      IF(D2(NG) .LE.RMIN(NX)) GO TO 201
      GO TO 200
  201 RMIN(NX) =  SQRT(D2(NG))
      XNAME(NX)= ANAME(NG)
  200 CONTINUE
  300 CONTINUE
      WRITE(6,301)(XNAME(NX),NX=1,5)
  301 FORMAT(1HT, 7H.      , 5(A6,4X), 3H  .)
      WRITE(6,302) (RMIN(NX),NX=1,5)
  302 FORMAT( 3H.  , 5F10.4 , 7H      .)
      WRITE(6,303)
  303 FORMAT(1HT, 1H., 58X, 1H.)
  400 CONTINUE
      WRITE(6,401)(SYMBOL(L),L=1,60)
  401 FORMAT(1HT,  60A1)
      GO TO 1000
      RETURN
      END
 ?32               PRECEDES B5000 AND IBJOB DATA CARDS
```

Sum of Probabilities Method of Classification

In order to account for the variation between deviations within six bands, a statistical method of multivariate analysis appears to give the best results. By using this program, the probability that an unknown spectrum may belong to a group is computed for each band by assuming that this is a function of a normal error curve. The position and shape of this curve is determined by the mean and standard deviation of the ideal groups in each of the six bands, and the probabilities are summed for each of the major groups being considered. For this purpose the error function ERF is called from the library of mathematical functions and suitably modified.

The input for the program consists of data cards of 45 spectra arranged as first described in this writeup. The output is a map of most probable spectra and their probabilities of being correct. A six-letter code word is printed along with the probability of its being the group selected as most likely, as the code words are input with the means and standard deviations by use of DATA statements.

Groups with extremely large standard deviations or an exceptionally large number of ideal spectra should be avoided, as the groups with the largest deviations will be chosen a disproportionate percent of the time.

```
$JOB   R563   IBJOB   2    800    BALLEW, GARY       233    SUM PROBS 4 POSS
$IBJOB
$IBFTC MAIN
C SUM OF PROBABILITIES MAP
      DIMENSION TITLE(12), SYMBOL(60),XNAME(5),BAND(5,9,6),
     1  SUM(3), AMEAN(4,6), SIGMA(4,6), ANAME(4)        ,RMAX(5)
      DATA  (ANAME(NG),NG=1,4) / 6HRHYOLT, 6HPUMICE, 6HSHADOW ,
     1  6HPUMISG /
      DATA  ((AMEAN(NG, I), I=1,6),NG=1,4) / 0.65167, 0.71111,  1.33167,
     1 1.82056, 1.19667,  2.64833,
     2  0.54696, 0.43913, 0.47870, 0.68239, 0.48196, 0.74174,
     3  0.40000, 0.27467,  0.31400, 0.45133, 0.35533, 0.52067,
     4  0.65270, 0.58919, 0.60635, 0.92770, 0.62703, 1.03851/
      DATA ((SIGMA(NG, I), I=1,6), NG=1,4) /  0.16745, 0.20041, 0.82748,
     1 0.68870, 0.51649, 1.47826,                                       SIG 1
     2 0.12811, 0.15430, 0.22833, 0.30602, 0.18508, 0.30488,            SIG 2
     3 0.11582, 0.12141, 0.23561, 0.27126, 0.16591, 0.43310 ,           SIG 3
     4  0.20135, 0.22041, 0.28852, 0.36734, 0.26782, 0.50920/           SIG 04
      DATA (SYMBOL(L)  ,L=1,60) / 60*1H./
 1000 READ(5,1)(TITLE(K),K=1,12)
    1 FORMAT(12A6)
      WRITE(6,2) (TITLE(K), K=1,12)
    2 FORMAT(1H1,12A6)
      WRITE(6,401)(SYMBOL(L),L=1,60)
      WRITE(6,303)
      WRITE(6,303)
      READ(5,3) (((BAND(NX,NY,I),I= 1,6), NY=1,9) ,NX=1,5)
    3 FORMAT (36X,6F4.2)
      DO 400 NY=1,9
      DO 300 NX=1,5
      RMAX(NX)=0.0
      DO 200 NG=1,4
      SUM(NG  ) = 0.0
      DO 100 I=1,6
      ABSDIF = ABS(BAND(NX,NY,I) - AMEAN(NG,I))
      SUM(NG) = SUM(NG) +(1.0 - ERF(ABSDIF / (SIGMA(NG,I) * 1.414214 )))
     1    /6.0
  100 CONTINUE
      IF(SUM(NG).GE.RMAX(NX)) GO TO 201
      GO TO 200
  201 RMAX(NX) = SUM(NG)
      XNAME(NX)= ANAME( NG)
  200 CONTINUE
  300 CONTINUE
      WRITE(6,301)(XNAME(NX),NX=1,5)
  301 FORMAT(1HT, 7H.      , 5(A6,4X), 3H  .)
      WRITE(6,302) (RMAX(NX),NX=1,5)
  302 FORMAT( 3H.  , 5F10.4 , 7H      .)
      WRITE(6,303)
  303 FORMAT(1HT, 1H., 58X, 1H.)
  400 CONTINUE
      WRITE(6,401)(SYMBOL(L),L=1,60)
  401 FORMAT(1HT,  60A1)
      GO TO 1000
      RETURN
```

```
       END
?32                     PRECEDES B5000 AND IBJOB DATA CARDS
```